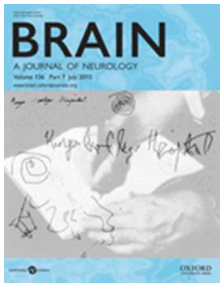

Human N-Methyl-D-aspartate receptor antibodies alter memory and behavior in mice

Journal:	*Brain*
Manuscript ID:	BRAIN-2014-00761.R1
Manuscript Type:	Original Article
Date Submitted by the Author:	11-Aug-2014
Complete List of Authors:	Planagumà, Jesús; Institut d'Investigacions Biomèdiques August Pi i Sunyer (IDIBAPS), Hospital Clínic, Neuroimmunology; The Institute of Photonic Sciences (ICFO), Advanced fluorescence imaging and biophysics Leypoldt, Frank; University Medical Center Schleswig-Holstein, Department of Neurology and Institute of Clinical Chemistry; Institut d'Investigacions Biomèdiques August Pi i Sunyer (IDIBAPS), Hospital Clínic, Neuroimmunology Mannara, Francesco; Institut d'Investigacions Biomèdiques August Pi i Sunyer (IDIBAPS), Hospital Clínic, Neuroimmunology; Universitat Pompeu Fabra, Ciències Experimentals i de la Salut Gutiérrez-Cuesta, Javier; Universitat Pompeu Fabra, Ciències Experimentals i de la Salut Martín-García, Elena; Universitat Pompeu Fabra, Ciències Experimentals i de la Salut Aguilar, Esther; Institut d'Investigacions Biomèdiques August Pi i Sunyer (IDIBAPS), Hospital Clínic, Neuroimmunology Titulaer, Maarten; Erasmus Medical Center, Department of Neurology Petit-Pedrol, Mar; Institut d'Investigacions Biomèdiques August Pi i Sunyer (IDIBAPS), Hospital Clínic, Neuroimmunology Jain, Ankit; University of Pennsylvania, Neurology Balice-gordon, Rita; University of Pennsylvania, Neurology Lakadamyali, Melike; The Institute of Photonic Sciences (ICFO), Advanced fluorescence imaging and biophysics Maldonado, Rafael; Universitat Pompeu Fabra, Ciències Experimentals i de la Salut Graus, Francesc; Institut d'Investigacions Biomèdiques August Pi i Sunyer (IDIBAPS), Hospital Clínic, Neuroimmunology; Hospital Clinic, Department of Neurology Dalmau, Josep; Institut d'Investigacions Biomèdiques August Pi i Sunyer (IDIBAPS), Hospital Clínic, Neuroimmunology; University of Pennsylvania, Neurology; Institució Catalana de Recerca i Estudis Avançats (ICREA), ,

Subject category:	Multiple sclerosis and neuroinflammation
To search keyword list, use whole or part words followed by an *:	Autoimmune encephalitis < MULTIPLE SCLEROSIS AND NEUROINFLAMMATION, Limbic encephalitis < MULTIPLE SCLEROSIS AND NEUROINFLAMMATION, Memory < DEMENTIA, Ion channels < SYSTEMS/DEVELOPMENT/PHYSIOLOGY, Synaptic transmission < SYSTEMS/DEVELOPMENT/PHYSIOLOGY

Human N-Methyl-D-aspartate receptor antibodies alter memory and behavior in mice

(Running head: Mouse model of anti-NMDA receptor encephalitis)

Jesús Planagumà PhD[1,2*], Frank Leypoldt MD PhD[1,3*], Francesco Mannara BS[1,4*], Javier Gutiérrez-Cuesta PhD[4], Elena Martín-García PhD[4], Esther Aguilar BS[1], Maarten J. Titulaer MD PhD[5], Mar Petit-Pedrol BS[1], Ankit Jain BS[6], Rita Balice-Gordon PhD[6], Melike Lakadamyali PhD[2], Francesc Graus MD[1,7], Rafael Maldonado PhD[4], and Josep Dalmau MD PhD[#1,8,9]

*contributed equally

1Institut d'Investigacions Biomèdiques August Pi i Sunyer (IDIBAPS), Hospital Clínic, Universitat de Barcelona, Barcelona, Spain

[2]ICFO-Institut de Ciències Fotòniques, Barcelona, Spain

[3]Institute of Clinical Chemistry, Neuroimmunology Unit, University Medical Center Schleswig-Holstein Campus Lübeck, Germany

[4]Laboratori de Neurofarmacología, Facultat de Ciències de la Salut i de la Vida, Universitat Pompeu Fabra, Barcelona, Spain

[5]Department of Neurology, Erasmus Medical Center, Rotterdam, the Netherlands

[6]Department of Neuroscience, University of Pennsylvania, PA, USA

[7]Servei de Neurología, Hospital Clínic, Universitat de Barcelona, Barcelona, Spain

[8]Department of Neurology, University of Pennsylvania, Philadelphia, PA, USA

[9]Institució Catalana de Recerca i Estudis Avançats (ICREA), Barcelona, Spain

[#] Corresponding author: Josep Dalmau, MD, PhD, IDIBAPS-Hospital Clínic, Universitat de Barcelona, Department of Neurology, c/ Villarroel 170, 08036, Barcelona, Spain. Phone: +34 932 271 738, e-mail: jdalmau@clinic.ub.es

Number of characters in title and running head: 80 and 46.

Number of words in the abstract: 399.

Number of words in the body of the manuscript: 5582.

Number of figures and tables: 8 (6 of them in color).

Supplementary information: text 1092 words, 2 Tables, and 2 Figures

Key words: Animal model, anti-NMDAR encephalitis, antibodies, pathogenesis, mechanism

Abstract

Anti-N-Methyl-D-aspartate receptor (NMDAR) encephalitis is a severe neuropsychiatric disorder that associates with prominent memory and behavioral deficits. Patients' antibodies react with the N-terminal domain of the GluN1 subunit of NMDAR causing in cultured neurons a selective and reversible internalization of cell-surface receptors. These effects and the frequent response to immunotherapy have suggested an antibody-mediated pathogenesis, but to date there is no animal model showing that patients' antibodies cause memory and behavioral deficits. To develop such a model, C57BL6/J mice underwent placement of ventricular catheters connected to osmotic pumps that delivered a continuous infusion of patients' or control cerebrospinal fluid (CSF, flow rate 0.25 µl/hour, 14 days). During and after the infusion period standardized tests were applied, including tasks to assess memory (novel object recognition in open field and V-maze paradigms), anhedonic behaviors (sucrose preference test), depressive-like behaviors (tail suspension, forced swimming tests), anxiety (black and white, elevated plus maze tests), aggressiveness (resident-intruder test), and locomotor activity (horizontal and vertical). Animals sacrificed at days 5, 13, 18, 26 and 46 were examined for brain-bound antibodies and the antibody effects on total and synaptic NMDAR clusters and protein concentration using confocal microscopy and immunoblot analysis. These experiments showed that animals infused with patients' CSF, but not control CSF, developed progressive memory deficits, and anhedonic and depressive-like behaviors, without affecting other behavioral or locomotor tasks. Memory deficits gradually worsened until day 18 (four days after the infusion stopped) and all symptoms resolved over the next week. Accompanying brain

tissue studies showed progressive increase of brain-bound human antibodies, predominantly in the hippocampus (maximal on days 13-18), that after acid-extraction and characterization with GluN1-expressing human embryonic kidney (HEK) cells were confirmed to be against the NMDAR. Confocal microscopy and immunoblot analysis of the hippocampus showed progressive decrease of the density of total and synaptic NMDAR clusters and total NMDAR protein concentration (maximal on day 18), without affecting the post-synaptic density protein (PSD)95 and α-Amino-3-hydroxy-5-methyl-4-isoxazolepropionic acid receptors (AMPAR). These effects occurred in parallel with memory and other behavioral deficits and gradually improved after day 18, with reversibility of symptoms accompanied by a decrease of brain-bound antibodies and restoration of NMDAR levels. Overall, these findings establish a link between memory and behavioral deficits and antibody-mediated reduction of NMDAR, provide the biological basis by which removal of antibodies and antibody-producing cells improve neurological function, and offer a model for testing experimental therapies in this and similar disorders.

Introduction

Memory, learning, and behavior depend on the proper function of the excitatory glutamate N-Methyl-D-aspartate receptor (NMDAR) and α-Amino-3-hydroxy-5-methyl-4-isoxazolepropionic acid receptor (AMPAR) and underlying mechanisms of synaptic plasticity (Lau and Zukin 2007; Shepherd and Huganir 2007). The critical role of NMDAR in these functions has been shown in animal models in which the NMDAR are altered genetically (Mohn *et al.* 1999; Belforte *et al.* 2010) or pharmacologically (Jentsch and Roth 1999; Mouri *et al.* 2007). In humans this evidence comes from more indirect observations such as studies investigating the effects of phencyclidine or ketamine (noncompetitive antagonists of NMDAR that cause psychosis) (Weiner *et al.* 2000; Gunduz-Bruce 2009), and brain tissue studies of patients with schizophrenia or Alzheimer's disease in which several molecular pathways that modulate glutamate receptor trafficking or function are affected (Hahn *et al.* 2006; Snyder *et al.* 2005). In 2007 we identified a novel disorder (anti-NMDAR encephalitis) that occurs with highly specific antibodies against extracellular epitopes located at the amino terminal domain of the GluN1 subunit of NMDAR (Dalmau *et al.* 2007; Gleichman *et al.* 2012). The resulting syndrome resembles the spectrum of symptoms that occurs in genetic or pharmacologic models of NMDAR hypofunction, including memory loss and neuropsychiatric alterations ranging from psychosis to coma (Dalmau *et al.* 2008; Viaccoz *et al.* 2014; Irani *et al.* 2010). Regardless of the type of presentation, most patients develop severe problems forming new memories and amnesia of the disease. Symptoms are usually accompanied by systemic and intrathecal synthesis of antibodies, the latter likely produced by plasma cells contained in brain inflammatory infiltrates (Dalmau *et al.* 2008; Martinez-Hernandez *et al.* 2011). These long-lived plasma cells and persistent antibody synthesis may explain the lengthy symptoms of most patients

(average hospitalization ~3 months) (Dalmau *et al.* 2008). Yet, despite the severity and duration of the disease, 80% of the patients have substantial recovery after immunotherapy (accompanied by removal of an underlying tumor, usually an ovarian teratoma, when appropriate), or sometimes spontaneously (Titulaer *et al.* 2013; Iizuka *et al.* 2008).

Investigations on the potential pathogenic role of patients' antibodies using cultured neurons showed that the antibodies caused crosslinking and selective internalization of NMDARs that correlated with the antibody titers, and these effects were reversible after removing the antibodies (Hughes *et al.* 2010; Mikasova *et al.* 2012). In contrast, patients' antibodies did not alter the localization or expression of other synaptic proteins, number of synapses, dendritic spines, dendritic complexity, or cell survival (Hughes *et al.* 2010). In parallel experiments, the density of NMDAR was also significantly reduced in the hippocampus of rats infused with patients' antibodies, a finding comparable to that observed in the hippocampus of autopsied patients (Hughes *et al.* 2010). Overall, these studies suggested an antibody-mediated pathogenesis, but the demonstration that patients' antibodies caused symptoms remained pending. Modeling symptoms and showing that these correlate with antibody-mediated reduction of NMDAR would prove the pathogenicity of patients' antibodies, support the use of treatments directed toward decreasing the levels of antibodies or antibody-producing cells, and help to investigate experimental therapies in this and similar disorders. We report here such a model using continuous 14-day cerebroventricular infusion of patients' CSF in mice. The aims were to determine 1) if patients' antibodies altered memory and behavior, 2) whether mice symptoms correlated with brain antibody-binding and reduction of NMDAR, and 3) whether the clinical and molecular alterations recovered after stopping the antibody infusion.

Methods

Animals

Male C57BL6/J mice (Charles River), 8-10 weeks old (25-30 g) were housed in cages of 5 until one week before surgery when they were housed individually. The room was maintained at a controlled temperature (21±1ºC) and humidity (55±10%) with illumination at 12 hour cycles; food and water were available *ad libitum*. All experiments were performed during the light phase, and animals were habituated to the experimental room for 1 week before starting the tests. All procedures were conducted in accordance with standard ethical guidelines (European Communities Directive 86/609/EU) and approved by the local ethical committees: Comitè Ètic d'Experimentació Animal, Institut Municipal d'Assistència Sanitària (Universitat Pompeu Fabra), and Instituional Animal Care and Use Committee (University of Pennsylvania).

Patients´ CSF samples

CSF from 25 patients with high titer NMDAR antibodies (all >1:320) were pooled and used for cerebroventricular infusion. CSF from 25 subjects without NMDAR antibodies (11 with normal pressure hydrocephalus and 14 with non-inflammatory CNS disorders) were similarly pooled and used as controls. Before loading the osmotic pumps (discussed below), the pooled CSF samples from patients and controls were dialyzed (Slide-A-Lyzer 7K, Thermo) against sterile phosphate buffered saline (PBS) overnight at 4°C, and the concentration of total IgG normalized to the CSF physiologic concentration of 2 mg/dL. All mice received the same pooled CSF either from patients or controls. Studies were approved by the institutional review board of Hospital Clínic

and Institut d'Investigacions Biomèdiques August Pi i Sunyer (IDIBAPS), Universitat de Barcelona.

Surgery, placement of ventricular catheters and osmotic pumps

Cerebroventricular infusion of CSF was performed using osmotic pumps (model 1002, Alzet, Cupertino, CA) with the following characteristics: volume 100 µl, flow rate 0.25 µl/hr, and duration 14 days. Twenty-four hours before surgery, two osmotic pumps per animal were each loaded with 100 µl of patients' or control CSF. The pumps were then connected to a 0.28 mm IM (internal diameter) polyethylene tube (C314CT, PlasticsOne) and left overnight in sterile phosphate buffered saline (PBS) at 37°C. The next day, mice were deeply anesthetized by intraperitoneal injection of a mixture of ketamine (100 mg per kg) and xylazine (10 mg per kg) along with subcutaneous administration of the analgesic meloxicam (1 mg per kg). Mice were then placed in a stereotaxic frame, and a bilateral catheter (PlasticsOne, model 3280PD-2.0/SP) was inserted into the ventricles (0.02 mm anterior and 1.00 mm lateral from bregma, depth 0.22 mm) and secured with dental cement. Each arm of the catheter was connected to one osmotic pump, which were subcutaneously implanted on the back of the mice. Appropriate ventricular placement of the catheters was assessed in randomly selected mice injecting methylene blue through the catheters (Figure 1A-C).

Cognitive tasks

All behavioral tasks were performed by researchers blinded to experimental conditions using standardized tests reported by us (Aso *et al.* 2008; Berrendero *et al.* 2005; Bura *et al.* 2013; Bura *et al.* 2007; Bura *et al.* 2010; Burokas *et al.* 2012; Filliol *et al.* 2000; Llorente-Berzal *et al.* 2013; Maldonado *et al.* 1970; Puighermanal *et al.* 2009) and

others (Taglialatela *et al.* 2009; Steru *et al.* 1985; Strekalova *et al.* 2006; Caille *et al.* 1999; Crawley and Goodwin 1980; Konig *et al.* 1996; Porsolt *et al.* 1977; Ennaceur 2010; Handley and Mithani 1984) and following the schedule summarized in Figure 1D. The tasks were aimed to assess memory (novel object recognition in open field and V-maze), anhedonic behaviors (sucrose preference test), depressive-like behaviors (tail suspension, and forced swimming tests), anxiety (black and white and elevated plus maze tests), aggressiveness (resident-intruder test) and locomotor activity (horizontal and vertical activity assessment). A brief description of each task is shown in supplemental material.

Brain tissue processing

To determine the effects of patients' antibodies on mouse brain, animals were sacrificed at the indicated time points (Figure 1D, Days 5, 13, 18, 26 and 46) with CO_2. Brains were harvested, sagittally split, and transferred to ice-cold PBS. Half of the brain was fixed by immersion in 4% paraformaldehyde (PFA) for 1 hour at 4°C, cryoprotected with 40% sucrose for 48 hours at 4°C, embedded with freezing media, and snap frozen with isopentane chilled with liquid nitrogen. The other half brain was used for dissection of hippocampus and cerebellum for IgG and protein extraction (see below).

Immunohistochemistry and quantitative peroxidase staining

For determination of antibodies bound to brain tissue using immunoperoxidase staining, 7 µm-thick tissue sections were sequentially incubated with 0.25% H_2O_2 for 10 minutes at 4°C, 5% goat serum for 15 minutes at room temperature (RT), biotinylated goat anti-human IgG (1:2000, Vector labs, Burlingame, CA, USA) overnight at 4°C, and the reactivity developed using avidin-biotin-peroxidase and diaminobenzidine. Sections

were mildly counterstained with hematoxylin, and results photographed under a Leica DMD108 microscope (Mannheim, Germany). Images were prepared creating a mask for diaminobenzidine color, converting the mask to grey scale intensities, and inverting the pixels using Adobe Photoshop CS6 package. Hippocampal, frontal cortex, striatum and cerebellar regions were manually outlined; intensity and area were quantified in two serial sections using the public domain Fiji ImageJ software (http://fiji.sc/Fiji). Values were divided by area and normalized to the group with the highest mean (defined as 100%, patients' CSF treated animals sacrificed at day 18).

Immunofluorescence and confocal microscopy with brain tissue

For determination of antibodies bound to brain tissue using immunofluorescence, 5 µm-thick tissue sections were blocked with 5% goat serum and 1% bovine serum albumin (BSA) for 60 minutes at RT, and incubated overnight at 4°C with Alexa Fluor 488 goat anti-human IgG (A11013, diluted 1:1000, Molecular Probes/ Life Technologies, Carlsbad, CA, USA). Slides were then mounted with ProlonGold (P36930, Molecular Probes) and results scanned under a LSM710 Zeiss confocal microscope. Sections from all animals were analyzed in parallel. Quantification of fluorescent intensity in areas of CA1, CA3 and DG was done using Fiji ImageJ software. Background was subtracted and intensity divided by area. Mean intensity of IgG immunostaining in animals treated with patients' CSF and sacrificed at day 18 was defined as 100%.

To determine the effects of patients' antibodies on total and synaptic NMDAR clusters and PSD95, non-permeabilized 5 µm-thick sections were blocked with 5% goat serum and 1% BSA as above, incubated with human CSF antibodies for 2 hours at RT, washed with PBS, permeabilized with Triton 0.3% for 10 minutes at RT, and incubated with rabbit polyclonal antibody against PSD95 (diluted 1:250, Clone 18258 Abcam,

Cambridge, UK) overnight at 4°C. Next day, the slides were washed and incubated with the corresponding secondary antibodies, Alexa Fluor 594 goat anti-human IgG and Alexa Fluor 488 goat anti-rabbit IgG (A-11014, A-11008, both diluted 1:1000, Molecular Probes) for 1 hour at RT. Slides were mounted as above and results scanned with a confocal microscope (Zeiss LSM710) with EC-Plan NEOFLUAR CS 100x/1.3 NA oil objective. Standardized z-stacks including 50 optical images were acquired from five different, equally spaced areas of CA1, CA3, and dentate gyrus (DG) of hippocampus using sequential scanning, 1024×1024 lateral resolution, and Nyquist optimized z sampling frequency. Images were deconvolved with 20 iterations using theoretical point spread functions and maximum likelihood estimation algorithms of Huygens Essential software (Scientific Volume Imaging BV, Hilversum, the Netherlands). For cluster density analysis a spot detection algorithm from Imaris suite 7.6.4 (Bitplane, Zurich, Switzerland) was used based on automatic segmentation of the images to spots (Banovic *et al.* 2010). Density of clusters was expressed as spots/µm3. Three-dimensional colocalization of clusters (e.g. NMDAR and PSD95) was done using a spot-colocalization algorithm implemented in Imaris suite 7.6.4. Synaptic localization was defined as colocalization of NMDAR or AMPAR with postsynaptic PSD95. Synaptic cluster density was expressed as colocalized spots/µm3. For each animal, five identical image stacks in each hippocampal area (CA1, CA2 and DG) were acquired and the mean densities calculated for total and synaptic NMDAR and AMPAR. Densities were normalized to the mean density of control CSF treated animals (100%). Antibodies used were guinea pig GluA1 antibody (1:100, clone AGP-009, Alomone, Jerusalem, Israel), and as secondary antibody Alexa Fluor 594 goat anti-guinea pig IgG (A11076, 1:1000, Molecular Probes).

The presence of apoptosis, cellular infiltrates, and complement was assessed in the hippocampal region (CA3) in mice sacrificed on day 18 and corresponding controls. Apoptosis was determined by standard terminal deoxynucleotidyl transferase mediated biotinylated UTP nick end labeling (TUNEL) using the TACS 2TdT-Fluor in situ apoptosis detection kit (Trevigen, Gaithersburg, MD, USA), and immunolabeling of cleaved caspase 3 (1:200, #9661 Cell Signalling, Technologies, Danvers, MA, USA) using a goat anti rabbit – Alexa 488 as secondary antibody (1:1000 Molecular Probes). The presence of complement was assessed using rabbit anti-mouse C5b-9 (1:500, Abcam) and Alexa Fluor 488 goat anti-rabbit IgG (1:500, #A11008, Molecular Probes). Immunolabeling for B- and T lymphocytes was done using rabbit anti-mouse CD3 (1:1000, #ab16669 Abcam) followed by secondary antibody goat anti-rabbit Alexa Fluor 488 (1:1000, Molecular Probes), and rat anti-CD45R (1/10000, #ab64100) followed by goat anti-rat Alexa Fluor 594 (1/1000, #A-11007 Molecular Probes). Results were scanned with a confocal microscope Zeiss LSM710.

Extraction of human IgG bound to mice brain

Under a dissection microscope (Zeiss stereomicroscope, Stemi 2000), the hippocampus and cerebellum were isolated, weighed, snap frozen, and stored at -80°C. Tissue (10 mg) was homogenized in 0.5 ml ice-cold PBS with protease inhibitors (Sigma-Aldrich, St. Louis, MO, USA) and centrifuged at 16.000g for 5 minutes. All steps were performed at 4°C. Washing was repeated four times to remove unbound IgG. The last wash was done in 100µl and the supernatant saved as pre-extraction fraction. To extract the specifically bound antibodies, the pellet was solubilized for 5 minutes in acid (86µl 0.1M Na-citrate buffer pH2.7), centrifuged at 16.000g for 5 minutes, and the

supernatant neutralized with 14µl 1.5M Tris pH8.8, and used to determine the presence of NMDAR (GluN1) antibodies (see below).

Immunofluorescence with HEK293 cells expressing GluN1

The presence of GluN1 antibodies in IgG extracts from brain was determined using a HEK293 cell-based assay expressing GluN1, as reported (Dalmau *et al.* 2008). After fixation with 4% PFA and permeabilization with 0.3% Triton X-100, cells were blocked with 1% BSA for 90 minutes, and incubated with undiluted acid-extracted IgG or pre-extraction fraction from brain of infused mice, at 4°C overnight. The next day, cells were washed and incubated with a mouse monoclonal antibody against a non-competing GluN1 epitope located at amino acid 660-811 (1:20.000; clone MAB363, Millipore) for 1 hour at RT, followed by the corresponding Alexa Fluor secondary antibodies (A11013, A11032, both diluted 1:1000, Molecular Probes) for 1 hour at RT. The titer of positive samples was calculated by serial dilutions until the reactivity was no longer visible. Results were photographed under a fluorescence microscope using Zeiss Axiovision software.

Immunoblot analyses

Total protein from hippocampus and cerebellum was obtained by dissecting these regions from 20 µm-thick PFA-fixed sagittal mouse brain sections on glass slides at 4°C under a Zeiss stereomicroscope (Stemi 2000). Two consecutive sections of isolated hippocampus or cerebellum were then transferred to an Eppendorf tube in PBS supplemented with protease inhibitors. Loading buffer (RotiLoad, Roth, Karlsruhe, Germany) was added, the solubilized tissue boiled for 5 minutes, and the proteins separated in a 10% SDS gel electrophoresis with semi-dry blotting on PVDF

membranes. Membranes were blocked in 5% non-fat skim milk and incubated overnight at 4°C with the following polyclonal rabbit antibodies: GluN1 (1:1000, Sigma-Aldrich), GluR2/3 (1:1000, Abcam), and PSD95 (1:1000, Synaptic Systems, Goettingen, Germany), or a monoclonal mouse anti-β-actin (1:20.000, Sigma-Aldrich). Membranes were incubated with secondary antibodies for 1 hour at RT (anti-rabbit-IgG-HRP 1:1000, anti-mouse-IgG-HRP 1:10.000) and analyzed by enhanced chemiluminescence (all Amersham-GE Healthcare, Pittsburgh, PA, USA) on a LAS4000 (GE Healthcare, Pittsburgh, PA, USA). All studies were done in duplicate. Analyzed films were in the linear range of exposure, digitally scanned, and signals quantified using Fiji ImageJ software. The signal intensity of each antigen was normalized to that of actin in the same lane. The mean intensity of signal in control CSF treated animals was defined as 100% and all other intensities expressed in percent relative to this value.

Statistics

Behavioral tests were analyzed using repeated measures two-way ANOVA for tests with multiple time points (novel object recognition, sucrose preference test, resident-intruder test, locomotor activity), independent sample-t tests for tests with single time-points (forced swimming test, black and white test, elevated plus maze test) or by Mann Whitney U for skewed distributions (tail suspension test). Non-normally distributed parameters were log-transformed (black and white test, elevated plus maze test). Significance of NMDAR antibody titer in acid-extracted IgG fractions was calculated using the Kruskal-Wallis test and Dunn's post-hoc test compared to titers at day 46. Human IgG intensity, confocal cluster density and immunoblot data (GluN1/PSD95) from different time points or regions were analyzed using two-way ANOVA with Sidak-Holm post-hoc testing to calculate multiplicity-adjusted p-values. Confocal

cluster density in the different hippocampal subregions (CA1, CA3, DG) were not significantly different and were analyzed pooled. All experiments were assessed visually for outliers (e.g., one animal with very different results from the other animals at the same time point), but none were identified, so measurements were pooled per time point and treatment (patient or control CSF). For confocal AMPAR cluster density measured at single time points, independent sample-t tests were used. A p-value of < 0.05 was considered significant in post-hoc testing after correction for multiple testing (Sidak-Holm). In the two-way ANOVA the cut-off for interaction between 2 factors was set at 0.10; if the p-value for interaction was < 0.10, the effects of treatment were considered for the separate time points (post-hoc analysis). All tests were done using GraphPad Prism (Version 6, La Jolla, CA, USA).

Results

One-hundred and eleven mice were included in the studies, 56 for cognitive and behavioral tests, and 55 for assessment of antibody binding to brain and the effects on total and synaptic NMDAR (Figure 1).

Cerebroventricular infusion of patients' CSF alters memory and behavior in mice

The most robust effect during the 14-day infusion of patients' CSF was on the novel object recognition test in both the open field and V-maze paradigms (Figure 2A,B). Compared with animals infused with control CSF, those infused with patients' CSF showed a progressive decrease of the object recognition index, indicative of a memory deficit (Bura *et al* 2007; Taglialatela *et al*. 2009; Puighermanal *et al*. 2009). The memory deficit became significant on day 10 and was maximal on day 18 (four days after the infusion of CSF had stopped). On day 25, the object recognition index had

normalized and was similar to that of animals treated with control CSF (Figure 2A,B). For all time-points, the total time spent exploring both objects (internal control) was similar in animals infused with control or patients' CSF (Supplemental Table 1).

The preference to drink sweetened water (sucrose preference test) was used as a measure of anhedonic behavior. Mice infused with patients' CSF and tested during the infusion period (day 10) had less preference for sucrose compared with mice infused with control CSF (Figure 2C). In contrast, the same mice tested 10 days after the infusion of CSF had stopped (day 24) showed a preference for sucrose similar to that of the control mice. The total consumption of water with and without sucrose was similar in both groups (internal control, Supplemental Table 1). In addition, two tests of depressive-like behavior were performed. The tail-suspension test, performed on day 12, showed that animals infused with patients' CSF had longer periods of immobility compared with those infused with control CSF (Figure 2D). In contrast, six days after the infusion of CSF had stopped (day 20), no differences were noted with the forced swimming test (examining immobility in inescapable situations; Figure 2E, Supplemental Table 1). Overall, these findings suggest that the infusion of NMDAR antibodies was associated with anhedonic and depressive-like behaviors.

In contrast to the prominent memory deficit, along with anhedonia and depressive behavior, no significant differences were noted in tests of anxiety (black and white test, elevated plus maze test), aggression (resident-intruder test) and locomotor activity (Figure 3A-D).

Patients' antibodies bind to NMDAR in mouse brain

Animals infused with patients' CSF, but not control CSF, had progressively increasing human IgG immunostaining (representing IgG bound to brain) that correlated with the

duration of the infusion. The distribution of IgG immunostaining predominated in regions with high density of NMDAR, mainly the hippocampus (Figure 4A), resembling that obtained with brain sections directly incubated with patients' CSF or a monoclonal antibody against GluN1 (Dalmau *et al.* 2008). Upon quantification of immunostaining, the maximal antibody binding was identified in mice sacrificed on day 18, which had received 14 days of CSF infusion, compared with mice sacrificed on days 5 or 13 (Figure 4B,C). In animals sacrificed on days 26 and 46 the presence of IgG immunostaining progressively decreased. In frontal cortex the dynamics of IgG binding were similar to those of the hippocampus (Supplemental Figure 1), but the amount of IgG was substantially less; in other brain regions such as the cerebellum and striatum, the IgG immunostaining was sparse and not significantly different between animals infused with patients' CSF or control CSF (data not shown).

Studies with immunofluorescence and confocal microscopy showed that in animals infused with patients' CSF the presence of hippocampal IgG was visible as a punctate immunolabeling on the surface of neurons and neuronal processes in contrast to mice infused with control CSF where minor amounts of IgG reactivity without preference for neuronal structures were noted (Figure 4D-G). In addition, the amount of human IgG bound to all selected regions of hippocampus was significantly higher than in the control group (Figure 4H).

To determine if the IgG immunostaining represented brain-bound NMDAR antibodies, IgG was extracted from several brain regions and examined for reactivity with HEK cells expressing GluN1. These studies showed that the IgG extracted from hippocampus of mice infused with patients' CSF reacted specifically with GluN1 (Figure 5A). The NMDAR antibody concentration in the extracts correlated with the duration of infusion of CSF; it increased until day 13, reached the maximal

concentration on days 13-18, and decreased afterwards (Figure 5A,C). NMDAR antibodies were also detected in IgG extracts from other brain regions (frontal cortex, cerebellum) but at lower concentration to that obtained from hippocampus (Figure 5D). Demonstration that the extracted antibodies were specifically bound to the NMDAR was provided by the lack of GluN1 reactivity in the pre-extraction fractions (Figure 5B,E). Parallel studies with tissue from animals infused with control CSF did not show NMDAR antibodies (Supplemental Figure 2).

Patients' antibodies cause a decrease of the density of NMDAR clusters and total NMDAR protein in mice hippocampus

To determine the effects of patients' antibodies on NMDAR, we focused on the hippocampus, which was the region with maximal concentration of NMDAR-bound antibodies. Compared with animals infused with control CSF those infused with patients CSF had on days 13 and 18 a significant decrease of the density of total and synaptic hippocampal NMDAR clusters followed by a gradual recovery after day 18 (pooled analysis of CA1, CA3 and DG, Figure 6A-D). No significant differences in between hippocampal subregions (CA1, CA3, DG) were observed (not shown). In contrast, patients' antibodies did not alter the density of PSD95 or AMPAR clusters (Figure 6E,F).

Immunoblot analysis of total protein extracted from hippocampus showed that on day 13 and 18, mice infused with patients' CSF had a significant decrease of total NMDAR protein concentration compared with mice infused with control CSF (Figure 7A,B). The magnitude of this effect was greater in animals with higher concentration of IgG bound to hippocampus (Figure 7C). Parallel studies examining the effect on the

protein concentrations of PSD95 (Figure 7A,E) and AMPAR (Figure 7D) demonstrated no significant differences between mice infused with patients' CSF or control CSF.

In cerebellum, no significant effects on the cluster density or total protein concentration of NMDAR, PSD95 and AMPAR were noted in animals infused with patients' CSF compared to those infused with control CSF (data not shown).

Immunohistochemical studies for neuronal apoptosis, infiltrates of T- or B-cells, and deposits of complement in hippocampus of animals infused with patients' or control CSF, examined on day 18, showed no abnormalities (Figure 8).

Discussion

We report that passive transfer of NMDAR antibodies by continuous ventricular infusion of CSF from patients with anti-NMDAR encephalitis causes memory and behavioral deficits in mice, and that the effects are likely mediated by the binding of antibodies to NMDAR resulting in a specific decrease of the density of these receptors. Data from earlier reports showing that despite the severity and duration of symptoms most patients with anti-NMDAR encephalitis respond to immunotherapy (Gresa-Arribas *et al.* 2013), and findings at the cellular level demonstrating that patients' antibodies cause a titer-dependent decrease of synaptic NMDAR receptors fulfilled most of the Witebsky's criteria for an antibody-mediated disease (Rose and Bona 1993), but the transfer of symptoms to animals was pending. In the current study, four sets of experiments satisfy this postulate, 1) the development of symptoms in animals infused with patients' CSF, but not control CSF, 2) the demonstration that the infused antibodies reacted predominantly with brain regions with high density of NMDAR (e.g., hippocampus) and specifically recognized these receptors, 3) the identification of a

selective decrease of the density of total and synaptic NMDAR clusters and total NMDAR protein concentration without affecting PSD95, and that these effects correlated with the concentration of brain-bound antibodies, and 4) the correlation noted between the intensity of the above-mentioned findings and time-course of patients' antibody infusion, as well as between the reversibility of symptoms and restoration of NMDAR levels after stopping the infusion of CSF antibodies.

Approximately 75% of patients with anti-NMDAR encephalitis present with mood and psychiatric alterations ranging from manic or depressive behavior to psychosis, often followed by stereotyped movements, seizures, or decreased level of consciousness (Titulaer *et al.*2013;Kayser *et al.* 2013). Regardless of the presentation, most patients develop severe problems forming new memories and have amnesia of the disease. Close examination during the phase of recovery shows in some patients impairment in the visual recognition of objects or faces (e.g., physicians, nurses) (Frechette *et al.* 2011). Owing to the wide range of symptoms of the disease and lack of previous studies examining the distribution of brain tissue NMDAR-antibody binding when these antibodies are infused intraventricularly, we used standardized memory and behavioral tests. The most notable effects were observed in the tests of memory (novel object recognition) using different groups of animals in two different paradigms (open field and V-maze). While the first depends predominantly on normal hippocampal function, the second is dependent of perirhinal-hippocampal structures (Winters *et al.* 2004). Compared with animals infused with control CSF, those infused with patients' CSF developed progressive memory deficits, which were maximal on days 13-18 when the highest concentration of brain-bound NMDAR antibodies and lowest density of NMDAR occurred. Other paradigms affected were related to depressive-like behaviors (tail suspension test) and anhedonic behaviors (sucrose preference test). We did not find

significant abnormalities in the tests of aggression and anxiety, which are often present in the human disease, or in locomotor activity (an expected finding given that paralysis rarely occurs in patients).

The high levels of brain-bound NMDAR antibodies between days 13-18 suggests that after stopping the infusion of patients' CSF on day 14, the NMDAR antibodies continued being distributed from mice cerebroventricular system to parenchyma. This distribution occurred slowly; for example, five days after starting the infusion of patients' CSF the amount of NMDAR antibodies that had reached the hippocampus was very limited compared to that seen on days 13-18 (shown in Figure 4B). Moreover, previous studies using cultured neurons treated with patients' CSF showed that once the antibodies bound to the NMDARs, the reduction of receptors was microscopically visible in two hours but it took 12 hours to result in the lowest receptor density. Subsequently, there was a steady state of low NMDAR density for as long as the neurons were exposed to patients' antibodies (Moscato *et al.* 2014). Together, these findings explain the progressive worsening of symptoms along with continued antibody binding and decrease of NMDAR for at least 4 days after the ventricular infusion stops and the subsequent recovery starts.

Although the hippocampus was the region with the highest concentration of brain-bound NMDAR antibodies, these antibodies were also extracted from cerebral cortex or cerebellum though at much lower levels. The higher concentration of antibodies and predominant decrease of NMDAR in the hippocampus are consistent with the predominant binding of human antibodies to this brain region when sections of rodent brain are directly incubated with patients' antibodies (Dalmau *et al.*, 2007; Moscato *et al.* 2014). Additionally, because of the close spatial relationship to the

ventricles, the intraventricular infusion of human CSF antibodies might have contributed to the preferential binding to the hippocampus.

The correlation between the concentration of brain-bound antibodies and selective reduction of NMDAR cluster density and protein concentration was similar to that reported using *in vitro* studies with cultured rat hippocampal neurons (Hughes *et al.,* 2012; Moscato *et al.* 2014). Moreover, autopsies of patients with anti-NMDAR encephalitis showed that the hippocampal regions with highest concentration of brain-bound antibodies were also the areas with lower expression of NMDAR (Dalmau *et al.,* 2007). In the current model, patients' antibodies did not alter AMPAR cluster density or protein concentration; these findings are in line with those reported with cultured neurons where the clusters of AMPAR and AMPAR-mediated currents were not directly affected (Hughes *et al.,* 2010). These experiments, however, did not explore whether paradigms, that normally induce long-term potentiation, and therefore increase the number of synaptic AMPAR, were altered by patients' antibodies. Mikasova and colleagues showed that neurons exposed to patients' NMDAR antibodies failed to show an increase in cell surface AMPAR after induction of chemical long-term potentiation (Mikasova *et al.,* 2012). Another study examining the acute metabolic effects of patients' antibodies after injection into rat brain showed impairment of NMDA and AMPA-mediated synaptic function (Manto *et al.* 2010). In the present model, we did not perform electrophysiological studies on acute slices of brain (a goal of future studies); however, there is reported evidence that patients' NMDAR antibodies suppress induction of long-term potentiation when directly applied to mouse hippocampal slices (Zhang *et al.* 2012). Work with cultured neurons indicates that the decrease of synaptic NMDAR currents is likely a result of the antibody-mediated low receptor levels, as no direct antibody blockade was detected (Moscato *et al.* 2014).

Our study has limitations related to the type of disease and symptoms to model. For example, different from other models of antibody-mediated CNS disorders where the antibodies result in characteristic symptoms (e.g., amphiphysin antibodies and visible muscle spasms) (Sommer *et al.* 2005) or focal deficits with visible tissue changes (e.g., aquaporin4 antibodies and neuromyelitis optica) (Hinson *et al.* 2012;Bradl and Lassmann 2014), anti-NMDAR encephalitis results in a broader spectrum of symptoms where memory and behavioral deficits occur early, and the structural alterations are not visible unless the NMDAR clusters or protein concentration are measured. It is not surprising that in the current model the full spectrum of symptoms, such as seizures, dyskinesias or coma, did not occur. Studies with NMDAR antagonists have shown that the progression of symptoms (from behavioral and memory deficits to unresponsiveness with catatonic features and coma) correlated with the intensity of the decrease of receptor function (Javitt and Zukin 1991). Therefore, it is likely that prolonged infusion or higher concentration of patients' antibodies would cause additional symptoms. This is supported by the current model, in which the time course of symptom development, brain-bound antibody concentration, and decrease of synaptic NMDAR correlated well with each other. Future experiments using prolonged infusion or higher concentration of patients' antibodies may also result in symptoms beyond hippocampal-parahippocampal regions. Compared with the hippocampus, other brain regions normally have lower density of NMDAR, and appeared to be less accessible to the ventricularly infused antibodies. Direct injection of antibodies into those brain regions can be considered, but we previously tried bilateral hippocampal infusion using the same osmotic pump approach, resulting in more limited antibody diffusion and no symptoms (A Jain et al, data not published). Moreover, the phenotype of the current model is likely influenced by the strain of mice. In this study

we used C57BL6/J mice because we were interested in the effects on memory and behavior, but this strain is one of the most resistant to develop seizures (Ferraro *et al.* 2002).

The antibody-induced depletion of synaptic NMDAR along with the similarities between the human disease and the phenotypes induced by NMDAR antagonists (phencyclidine, ketamine or MK801) have suggested points of convergence with one of the most influential theories of schizophrenia, the NMDA-hypofunction model (Olney and Farber 1995; Kehrer *et al.* 2008). The presence of positive (hallucinations, delusions, hyperactivity) and negative (decreased motivation, flat affect, deficit of memory and learning) symptoms is however not identical among the drug-induced phenotypes and also varies among animal species (Javitt and Zukin 1991). It has been suggested that NMDAR-bearing parvalbumin positive GABAergic interneurons are disproportionally more sensitive to NMDAR antagonists than other neurons (Li *et al.* 2002). Interestingly, a genetic model of partial ablation of the GluN1 subunit of NMDAR in corticolimbic GABAergic interneurons resulted in symptoms partially resembling our GluN1 immunological model of receptor depletion, including memory deficits and anhedonic behaviors (Belforte *et al,* 2010) Differences related to the underlying mechanisms (pharmacologic blockade, genetic or immunologic NMDAR depletion) and regions where the NMDAR function is depleted (general, mesolimbic, or hippocampal-parahippocampal) likely influence the clinical phenotypes.

Overall, the current findings provide robust evidence that antibodies from patients with anti-NMDAR encephalitis alter memory and behavior through reduction of cell-surface and synaptic NMDAR, and therefore support the use of treatments directed at decreasing the levels of antibodies or antibody-producing cells. This approach can now be adapted to 1) model other aspects of the disease by changing the

duration and dosing of antibody infusion, or strain of mice, 2) investigate other disorders of memory and behavior that occur in association with antibodies against other cell surface or synaptic proteins, such as AMPAR or GABA(B)R (Lai *et al.* 2009; Lancaster *et al.* 2010), and 3) determine whether compounds such as Ephrin-B2 ligand that has been shown to prevent the destabilizing NMDAR crosslinking effects of patients' antibodies improve or alter the course of the disease (Mikasova *et al.,* 2012).

Acknowledgements

We thank Anna Planas and Vanessa Brait for providing stroke brain tissue and Jordi Andilla for technical support.

Study supported by: This work was supported by the National Institutes of Health RO1NS077851 (JD), RO1MH094741 (R. B-G and JD), Fundació La Marató de TV3 (JD), Fondo de Investigaciones Sanitarias/Instituto Carlos III (FIS PI11/01780 JD), ErasmusMC fellowship (MT), and Forschungsförderungsfonds Hamburg-Eppendorf FL).

Conflicts of interest: Dr. Dalmau holds a patent for the use of NMDA receptor as autoantibody test. Dr. Dalmau has received a research grant from Euroimmun Inc

Legends to Figures

Figure 1: Experimental design and placement of ventricular catheters

(A) Representative coronal mouse brain section with catheter placement. Scale bar=2 mm.

(B, C) Coronal and sagittal mouse brain sections demonstrating cerebroventricular diffusion of methylene blue after ventricular infusion. Scale bars=2 mm.

(D) Schedule of cognitive testing and animal sacrifice. At day 0, catheters and osmotic pumps were placed and bilateral ventricular infusion of patients' or control CSF started. Infusion lasted for 14 days. Memory (novel object recognition [NOR]), anhedonia (sucrose preference test [ANH]), depressive-like behavior (tail suspension test [TST] and forced swimming test [FST]), anxiety (black and white test [BW] and elevated plus maze test [EPM]), aggressiveness (resident intruder test [RI]) and locomotor activity (LOC) were assessed blinded to treatment at the indicated days. The NOR was assessed in open field and V-maze paradigms in two different cohorts of mice. Animals were habituated for 1 to 4 days before surgery (baseline) to NOR, ANH, and LOC. Red arrowheads indicate the days of sacrifice for studies of effects of antibodies in brain.

Figure 2: Infusion of CSF from patients with NMDAR antibodies causes deficits in memory, anhedonia, and depressive-like behavior

(A,B) Novel object recognition (NOR) index in open field (**A**) or V-maze paradigms. (**B**) in animals treated with patients' CSF (grey circles) or control CSF (white circles) A high index indicates better object recognition memory.

(C) Preference for sucrose-containing water in animals infused with patients CSF (grey) or control CSF (white). Lower percentages indicate anhedonia.

(D,E) Total time of immobility in tail-suspension test during the infusion period (**D**, day 12) and in forced swimming test after the infusion period (**E**, day 20). Data are presented as mean ± s.e.m (median ± IQR in **D).**

Number of animals: Patients' CSF n=18 (open field NOR n=8), control CSF n=20 (open field NOR n=10). Significance of treatment effect was assessed by two-way ANOVA (A-C) with an α-error of 0.05 and post-hoc testing with Sidak-Holm adjustment (asterisks), unpaired t-test (E) or Mann-Whitney U test (D). * P<0.05, *** P<0.001. See Supplemental Table 1 for detailed statistics.

Figure 3: Infusion of CSF from patients with NMDAR antibodies does not alter the tests of anxiety, aggression, and locomotor activity

(A, B) Number of entries into bright/open compartments during a five minute period in a standard black & white (**A,** day 6) or elevated plus maze test (**B,** day 14) in animals treated with patients' CSF (grey circles) or control CSF (white circles).

(**C**) Number of aggressive events over a four-minute period in a resident intruder paradigm in both treatment groups.

(**D**) Horizontal (solid lines) and vertical (dashed lines) movement count over a ten minute period in both treatment groups.

Data are presented as mean ± s.e.m**.** Number of animals: Patients' CSF n=18, control CSF n=20. Statistical assessment as indicated in Figure 2, and Supplemental Table 1.

Figure 4: Animals infused with patient's CSF have a progressive increase of human IgG bound to hippocampus

(A, B) Immunostaining of human IgG in sagittal brain sections (**A**) and hippocampus (**B**) of representative animals infused with patients' CSF (left panels) and control CSF (right panels), sacrificed at the indicated experimental days. In animals infused with patients' CSF there is a gradual increase of IgG immunostaining until day 18, followed by decrease of immunostaining. Scale bar in **A**=2 mm; scale bar in **B**=200 µm.

(C) Quantification of intensity of human IgG immunolabeling in hippocampus of mice infused with patients' CSF (grey columns) and control CSF (white columns) sacrificed at the indicated time points.

(D-H) Confocal microscopy analysis of IgG bound to the hippocampus on day 18. **(D)** Sagittal section of the hippocampus with areas examined at higher magnification in **E** (arrow in CA1), **F** (arrow heads in CA3) and **G** (asterisks in dentage gyrus [DG]). Note the fine punctate IgG immunolabeling surrounding neuronal bodies in mice infused with patients CSF; this immunolabeling is similar to that reported in brain sections directly incubated with patients' antibodies, as in (Dalmau *et al.* 2008). Scale bar in **D**=200 µm; scale bars in **E-G**=10 µm.

(H) Quantification of the intensity of human IgG immunofluorescence in the indicated areas in animals infused with patients' CSF (grey columns) or control CSF (white columns).

For all quantifications, mean intensity of IgG immunostaining in the group with the highest value (animals treated with patients' CSF and sacrificed at day 18) was defined as 100%. All data are presented as mean ± s.e.m. For each time point 5 animals infused with patients' CSF and 5 with control CSF were examined. Significance of treatment effect was assessed by two-way ANOVA with an α-error of 0.05 (*) and post-hoc testing with Sidak-Holm adjustment ($). ***, $$$ P<0.001; $, P<0.05. See Supplemental Table 2 for detailed statistics.

Figure 5: The human IgG extracted from brain of mice infused with patients' CSF is specific for NMDARs

(A,B) HEK293 cells expressing the GluN1 subunit of the NMDAR immunolabeled with acid-extracted IgG fractions (top row in **A**) or pre-extraction fractions (top row in **B**) from hippocampus of mice infused with patients' CSF and sacrificed on the indicated days. The maximal reactivity with GluN1-expressing cells was noted in acid-extracted IgG fractions from days 13 and 18 (**A**); none of the pre-extraction fractions showed GluN1 reactivity (**B**) indicating that the reactivity of acid-extracted fractions corresponds to IgG antibodies that were bound to brain NMDAR receptors. The second row in **A** and **B** shows the reactivity with a monoclonal GluN1 antibody, and the third row the co-localization of immunolabeling. Scale bars=10μm.

(C) Quantification of NMDAR antibody titer in IgG-extracted fractions from hippocampus of animals treated with patients' CSF (n= 5 mice per each time point, except 4 mice for day 5). Solid line = median. Significance was tested by Kruskal-Wallis with an α-error of 0.05 (asterisks) and post-hoc testing with Dunn's test ($). **,$$ P<0.01, ***,$$$ P<0.001. See Supplemental Table 2 for detailed statistics.

(**D, E)** HEK293 cells expressing the GluN1 subunit of the NMDAR immunolabeled with acid-extracted IgG fractions **(D)** and pre-extraction fractions **(E)** from hippocampus, cerebral cortex (Ctx) and cerebellum (Cb) of mice infused with patients' CSF (day 18). The acid-extracted IgG fraction from hippocampus showed higher level of NMDAR antibodies than those extracted from cerebral cortex (ctx) and cerebellum (Cb). Scale bars=10μm.

Figure 6: Patients' NMDAR antibodies selectively reduce the density of total and synaptic NMDAR clusters in hippocampus of mice

(A) Hippocampus of mice infused for 14 days (day 18) with patients' CSF (upper row) or control CSF (lower row) immunolabeled for PSD95 and NMDAR. Images were merged (merge) and post-processed to demonstrate co-localizing clusters (colocalization). Squares in "colocalization" indicate the analyzed areas in CA1, CA3 and DG. Scale bar=200 µm.

(**B**) 3D projection and analysis of the density of total clusters of PSD95 and NMDAR, and synaptic clusters of NMDAR (defined as NMDAR clusters colocalizing with PSD95) in a representative CA3 region (square in **A** "colocalization"). Merged images (merge, PSD95 green, NMDAR red) were post-processed and used to calculate the density of clusters (density=spots/μm^3). Scale bar=2 µm.

(C-F) Quantification of the density of total (**C**) and synaptic (**D**) NMDAR clusters, PSD95 clusters (**E**), and total/synaptic AMPAR clusters (day 18 only, **F**) in a pooled analysis of hippocampal subregions (CA1, CA3, DG) in animals treated with patients' CSF (grey) or control CSF (white) on the indicated days. Mean density of clusters in control CSF treated animals was defined as 100%. Data are presented as mean ± s.e.m. For each time point 5 animals infused with patients' CSF and 5 with control CSF were examined. Significance of treatment effect was assessed by two-way ANOVA with an α-error of 0.05 (asterisks) and post-hoc testing with Sidak-Holm adjustment ($) (C,D,E) or unpaired t-test (F). *,$ P< 0.05; **,$$ P< 0.01; ***,$$$ P<0.001. See Supplemental Table 2 for detailed statistics.

Figure 7: Patients' NMDAR antibodies selectively reduce the protein concentration of NMDAR in hippocampus of mice

A) Representative immunoblots of proteins extracted from hippocampus of animals infused with patients' CSF (P) or control CSF (C) sacrificed at the indicated time points and probed for expression of GluN1 (NMDAR), PSD95 and β-Actin (loading control). Note that there is less visible GluN1 expression on days 13 and 18.

(B, D, E) Quantification of total NMDAR **(B)**, PSD95 **(D)** or AMPAR (**E**) protein in animals treated with patients' CSF (grey columns) or control CSF (white columns) sacrificed at the indicated time points (AMPAR day 18 only, **E**). Results were normalized to β-Actin (loading control). Mean band density of animals treated with control CSF was defined as 100%. Data are presented as mean ± s.e.m. For each time point 6 animals infused with patients' CSF and 6 with control CSF were examined (for days 26 and 46, only 5 animals treated with patient's CSF were available). Significance of treatment effect was assessed by two-way ANOVA with an α-error of 0.05 (asterisks) and post-hoc testing with Sidak-Holm adjustment ($). $$ P< 0.01; *** P< 0.001. See Supplemental Table 2 for detailed statistics

(C) Correlation between concentration of human IgG bound to hippocampus (x-axis, highest hippocampal IgG intensity was defined as 100%) and hippocampal NMDAR protein concentration in mice sacrificed on day 18 (R^2=0.69, p=0.003). Grey circles: mice infused with patients' CSF (n=5), white circles: mice infused with control CSF (n=5).

Figure 8: Absence of neuronal apoptosis, deposits of complement, and lymphocytic infiltrates in the hippocampus of mice infused with patients' CSF

(A,B) TUNEL and cleaved caspase 3 immunolabeling of a representative area of CA3 (area with maximal IgG binding and lower NMDAR concentration) of an animal infused with patients CSF, showing lack of apoptotic cells. A section of the same region in an animal with transient middle cerebral artery occlusion (stroke model) shows apoptotic cells in the penumbra (panel on the left).

(C) Same CA3 region as in (**A**) immunostained for C5b-9 showing lack of deposit of complement. A section of the same region in the indicated stroke model shows presence of complement in the penumbra (panel on the left).

(D,E) Same CA3 region as in (**A**) immunostained for T (CD3) and B (CD45R) lymphocytes showing absence of inflammatory infiltrates. A section of spleen was used as control tissue showing the presence of CD3 (green) and CD45R (red) cells. Scale bar=10 μm. Total number of animals examined: patients' CSF n=5; control CSF n=5. Scale bars=20μm.

References

Aso E, Ozaita A, Valdizan EM *et al*. BDNF impairment in the hippocampus is related to enhanced despair behavior in CB1 knockout mice. J Neurochem 2008; 105: 565-572.

Banovic D, Khorramshahi O, Owald D *et al*. Drosophila neuroligin 1 promotes growth and postsynaptic differentiation at glutamatergic neuromuscular junctions. Neuron 2010; 66: 724-738.

Belforte JE, Zsiros V, Sklar ER *et al*. Postnatal NMDA receptor ablation in corticolimbic interneurons confers schizophrenia-like phenotypes. Nat Neurosci 2010; 13: 76-83.

Berrendero F, Mendizabal V, Robledo P *et al*. Nicotine-induced antinociception, rewarding effects, and physical dependence are decreased in mice lacking the preproenkephalin gene. J Neurosci 2005; 25: 1103-1112.

Bradl M, Lassmann H. Experimental models of neuromyelitis optica. Brain Pathol 2014; 24: 74-82.

Bura AS, Guegan T, Zamanillo D, Vela JM, Maldonado R. Operant self-administration of a sigma ligand improves nociceptive and emotional manifestations of neuropathic pain. Eur J Pain 2013; 17: 832-843.

Bura SA, Burokas A, Martin-Garcia E, Maldonado R. Effects of chronic nicotine on food intake and anxiety-like behaviour in CB(1) knockout mice. Eur Neuropsychopharmacol 2010; 20: 369-378.

Bura SA, Castane A, Ledent C, Valverde O, Maldonado R. Genetic and pharmacological approaches to evaluate the interaction between the cannabinoid and cholinergic systems in cognitive processes. Br J Pharmacol 2007; 150: 758-765.

Burokas A, Gutierrez-Cuesta J, Martin-Garcia E, Maldonado R. Operant model of frustrated expected reward in mice. Addict Biol 2012; 17: 770-782.

Caille S, Espejo EF, Reneric JP, Cador M, Koob GF, Stinus L. Total neurochemical lesion of noradrenergic neurons of the locus ceruleus does not alter either naloxone-precipitated or spontaneous opiate withdrawal nor does it influence ability of clonidine to reverse opiate withdrawal. J Pharmacol Exp Ther 1999; 290: 881-892.

Crawley J, Goodwin FK. Preliminary report of a simple animal behavior model for the anxiolytic effects of benzodiazepines. Pharmacol Biochem Behav 1980; 13: 167-170.

Dalmau J, Gleichman AJ, Hughes EG *et al*. Anti-NMDA-receptor encephalitis: case series and analysis of the effects of antibodies. Lancet Neurol 2008; 7: 1091-1098.

Dalmau J, Tuzun E, Wu HY *et al*. Paraneoplastic anti-N-methyl-D-aspartate receptor encephalitis associated with ovarian teratoma. Ann Neurol 2007; 61: 25-36.

Ennaceur A. One-trial object recognition in rats and mice: methodological and theoretical issues. Behav Brain Res 2010; 215: 244-254.

Ferraro TN, Golden GT, Smith GG, DeMuth D, Buono RJ, Berrettini WH. Mouse strain variation in maximal electroshock seizure threshold. Brain Res 2002; 936: 82-86.

Filliol D, Ghozland S, Chluba J *et al*. Mice deficient for delta- and mu-opioid receptors exhibit opposing alterations of emotional responses. Nat Genet 2000; 25: 195-200.

Frechette ES, Zhou L, Galetta SL, Chen L, Dalmau J. Prolonged follow-up and CSF antibody titers in a patient with anti-NMDA receptor encephalitis. Neurology 2011; 76: S64-S66.

Gleichman AJ, Spruce LA, Dalmau J, Seeholzer SH, Lynch DR. Anti-NMDA Receptor Encephalitis Antibody Binding Is Dependent on Amino Acid Identity of a Small Region within the GluN1 Amino Terminal Domain. J Neurosci 2012; 32: 11082-11094.

Gresa-Arribas N, Titulaer MJ, Torrents A *et al*. Antibody titres at diagnosis and during follow-up of anti-NMDA receptor encephalitis: a retrospective study. Lancet Neurol 2014; 13: 167-177.

Gunduz-Bruce H. The acute effects of NMDA antagonism: from the rodent to the human brain. Brain Res Rev 2009; 60: 279-286.

Hahn CG, Wang HY, Cho DS *et al*. Altered neuregulin 1-erbB4 signaling contributes to NMDA receptor hypofunction in schizophrenia. Nat Med 2006; 12: 824-828.

Handley SL, Mithani S. Effects of alpha-adrenoceptor agonists and antagonists in a maze-exploration model of 'fear'-motivated behaviour. Naunyn Schmiedebergs Arch Pharmacol 1984; 327: 1-5.

Hinson SR, Romero MF, Popescu BF *et al*. Molecular outcomes of neuromyelitis optica (NMO)-IgG binding to aquaporin-4 in astrocytes. Proc Natl Acad Sci U S A 2012; 109: 1245-1250.

Hughes EG, Peng X, Gleichman AJ *et al*. Cellular and synaptic mechanisms of anti-NMDA receptor encephalitis. J Neurosci 2010; 30: 5866-5875.

Iizuka T, Sakai F, Ide T *et al*. Anti-NMDA receptor encephalitis in Japan: long-term outcome without tumor removal. Neurology 2008; 70: 504-511.

Irani SR, Bera K, Waters P *et al*. N-methyl-D-aspartate antibody encephalitis: temporal progression of clinical and paraclinical observations in a predominantly non-paraneoplastic disorder of both sexes. Brain 2010; 133: 1655-1667.

Javitt DC, Zukin SR. Recent advances in the phencyclidine model of schizophrenia. Am J Psychiatry 1991; 148: 1301-1308.

Jentsch JD, Roth RH. The neuropsychopharmacology of phencyclidine: from NMDA receptor hypofunction to the dopamine hypothesis of schizophrenia. Neuropsychopharmacology 1999; 20: 201-225.

Kayser MS, Titulaer MJ, Gresa-Arribas N, Dalmau J. Frequency and characteristics of isolated psychiatric episodes in anti-N-methyl-d-aspartate receptor encephalitis. JAMA Neurol 2013; 70: 1133-1139.

Kehrer C, Maziashvili N, Dugladze T, Gloveli T. Altered Excitatory-Inhibitory Balance in the NMDA-Hypofunction Model of Schizophrenia. Front Mol Neurosci 2008; 1: 6.

Konig M, Zimmer AM, Steiner H *et al*. Pain responses, anxiety and aggression in mice deficient in pre-proenkephalin. Nature 1996; 383: 535-538.

Lai M, Hughes EG, Peng X *et al*. AMPA receptor antibodies in limbic encephalitis alter synaptic receptor location. Ann Neurol 2009; 65: 424-434.

Lancaster E, Lai M, Peng X *et al*. Antibodies to the GABA(B) receptor in limbic encephalitis with seizures: case series and characterisation of the antigen. Lancet Neurol 2010; 9: 67-76.

Lau CG, Zukin RS. NMDA receptor trafficking in synaptic plasticity and neuropsychiatric disorders. Nat Rev Neurosci 2007; 8: 413-426.

Li Q, Clark S, Lewis DV, Wilson WA. NMDA receptor antagonists disinhibit rat posterior cingulate and retrosplenial cortices: a potential mechanism of neurotoxicity. J Neurosci 2002; 22: 3070-3080.

Llorente-Berzal A, Puighermanal E, Burokas A *et al*. Sex-dependent psychoneuroendocrine effects of THC and MDMA in an animal model of adolescent drug consumption. PLoS ONE 2013; 8: e78386.

Maldonado JE, Kyle RA, Ludwig J, et al. Meningeal myeloma. Arch Intern Med 1970; 126: 660-663.

Manto M, Dalmau J, Didelot A, Rogemond V, Honnorat J. In vivo effects of antibodies from patients with anti-NMDA receptor encephalitis: further evidence of synaptic glutamatergic dysfunction. Orphanet J Rare Dis 2010; 5: 31.

Martinez-Hernandez E, Horvath J, Shiloh-Malawsky Y, Sangha N, Martinez-Lage M, Dalmau J. Analysis of complement and plasma cells in the brain of patients with anti-NMDAR encephalitis. Neurology 2011; 77: 589-593.

Mikasova L, De RP, Bouchet D *et al*. Disrupted surface cross-talk between NMDA and Ephrin-B2 receptors in anti-NMDA encephalitis. Brain 2012; 135: 1606-1621.

Mohn AR, Gainetdinov RR, Caron MG, Koller BH. Mice with reduced NMDA receptor expression display behaviors related to schizophrenia. Cell 1999; 98: 427-436.

Moscato EH, Peng X, Jain A, Parsons TD, Dalmau J, Balice-Gordon RJ. Acute mechanisms underlying antibody effects in anti-N-methyl-D-aspartate receptor encephalitis. Ann Neurol 2014; 76: 108-190.

Mouri A, Noda Y, Noda A *et al*. Involvement of a dysfunctional dopamine-D1/N-methyl-d-aspartate-NR1 and Ca2+/calmodulin-dependent protein kinase II pathway in

the impairment of latent learning in a model of schizophrenia induced by phencyclidine. Mol Pharmacol 2007; 71: 1598-1609.

Olney JW and Farber NB. Glutamate receptor dysfunction and schizophrenia. Arch Gen Psychiatry 1995; 52: 998-1007.

Porsolt RD, Bertin A, Jalfre M. Behavioral despair in mice: a primary screening test for antidepressants. Arch Int Pharmacodyn Ther 1977; 229: 327-336.

Puighermanal E, Marsicano G, Busquets-Garcia A, Lutz B, Maldonado R, Ozaita A. Cannabinoid modulation of hippocampal long-term memory is mediated by mTOR signaling. Nat Neurosci 2009; 12: 1152-1158.

Rose NR, Bona C. Defining criteria for autoimmune diseases (Witebsky's postulates revisited). Immunol Today 1993; 14: 426-430.

Shepherd JD, Huganir RL. The cell biology of synaptic plasticity: AMPA receptor trafficking. Annu Rev Cell Dev Biol 2007; 23: 613-643.

Snyder EM, Nong Y, Almeida CG *et al*. Regulation of NMDA receptor trafficking by amyloid-beta. Nat Neurosci 2005; 8: 1051-1058.

Sommer C, Weishaupt A, Brinkhoff J *et al*. Paraneoplastic stiff-person syndrome: passive transfer to rats by means of IgG antibodies to amphiphysin. Lancet 2005; 365: 1406-1411.

Steru L, Chermat R, Thierry B, Simon P. The tail suspension test: a new method for screening antidepressants in mice. Psychopharmacology (Berl) 1985; 85: 367-370.

Strekalova T, Gorenkova N, Schunk E, Dolgov O, Bartsch D. Selective effects of citalopram in a mouse model of stress-induced anhedonia with a control for chronic stress. Behav Pharmacol 2006; 17: 271-287.

Taglialatela G, Hogan D, Zhang WR, Dineley KT. Intermediate- and long-term recognition memory deficits in Tg2576 mice are reversed with acute calcineurin inhibition. Behav Brain Res 2009; 200: 95-99.

Titulaer MJ, McCracken L, Gabilondo I *et al*. Treatment and prognostic factors for long-term outcome in patients with anti-NMDA receptor encephalitis: an observational cohort study. Lancet Neurol 2013; 12: 157-165.

Viaccoz A, Desestret V, Ducray F *et al*. Clinical specificities of adult male patients with NMDA receptor antibodies encephalitis. Neurology 2014; 82: 556-563.

Weiner AL, Vieira L, McKay CA, Bayer MJ. Ketamine abusers presenting to the emergency department: a case series. J Emerg Med 2000; 18: 447-451.

Winters BD, Forwood SE, Cowell RA, Saksida LM, Bussey TJ. Double dissociation between the effects of peri-postrhinal cortex and hippocampal lesions on tests of object recognition and spatial memory: heterogeneity of function within the temporal lobe. J Neurosci 2004; 24: 5901-5908.

Zhang Q, Tanaka K, Sun P *et al*. Suppression of synaptic plasticity by cerebrospinal fluid from anti-NMDA receptor encephalitis patients. Neurobiol Dis 2012; 45: 610-615.

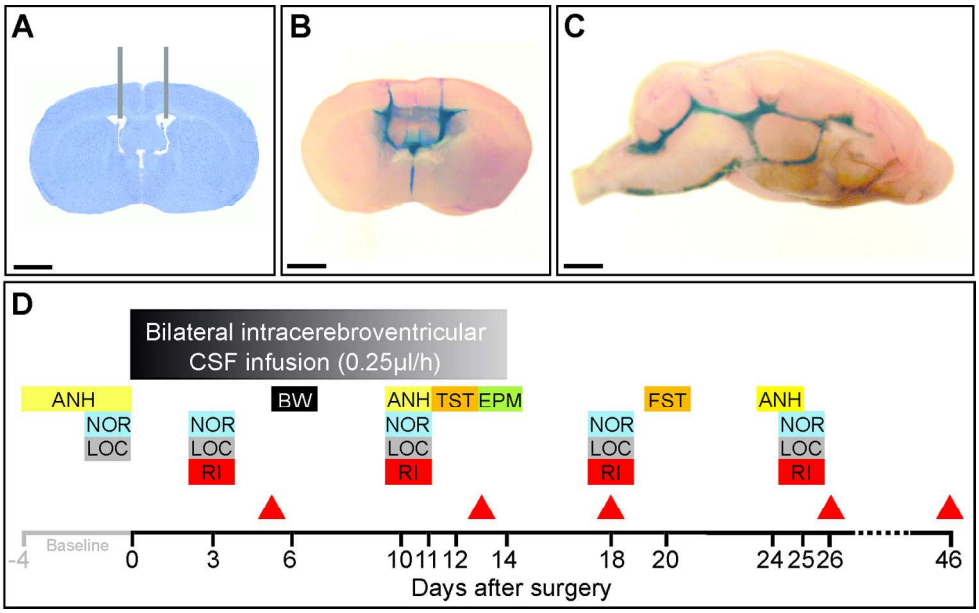

Figure 1: Experimental design and placement of ventricular catheters
(A) Representative coronal mouse brain section with catheter placement. Scale bar=2 mm.
(B, C) Coronal and sagittal mouse brain sections demonstrating cerebroventricular diffusion of methylene blue after ventricular infusion. Scale bars=2 mm.
(D) Schedule of cognitive testing and animal sacrifice. At day 0, catheters and osmotic pumps were placed and bilateral ventricular infusion of patients' or control CSF started. Infusion lasted for 14 days. Memory (novel object recognition [NOR]), anhedonia (sucrose preference test [ANH]), depressive-like behavior (tail suspension test [TST] and forced swimming test [FST]), anxiety (black and white test [BW] and elevated plus maze test [EPM]), aggressiveness (resident intruder test [RI]) and locomotor activity (LOC) were assessed blinded to treatment at the indicated days. The NOR was assessed in open field and V-maze paradigms in two different cohorts of mice. Animals were habituated for 1 to 4 days before surgery (baseline) to NOR, ANH, and LOC. Red arrowheads indicate the days of sacrifice for studies of effects of antibodies in brain.
155x93mm (300 x 300 DPI)

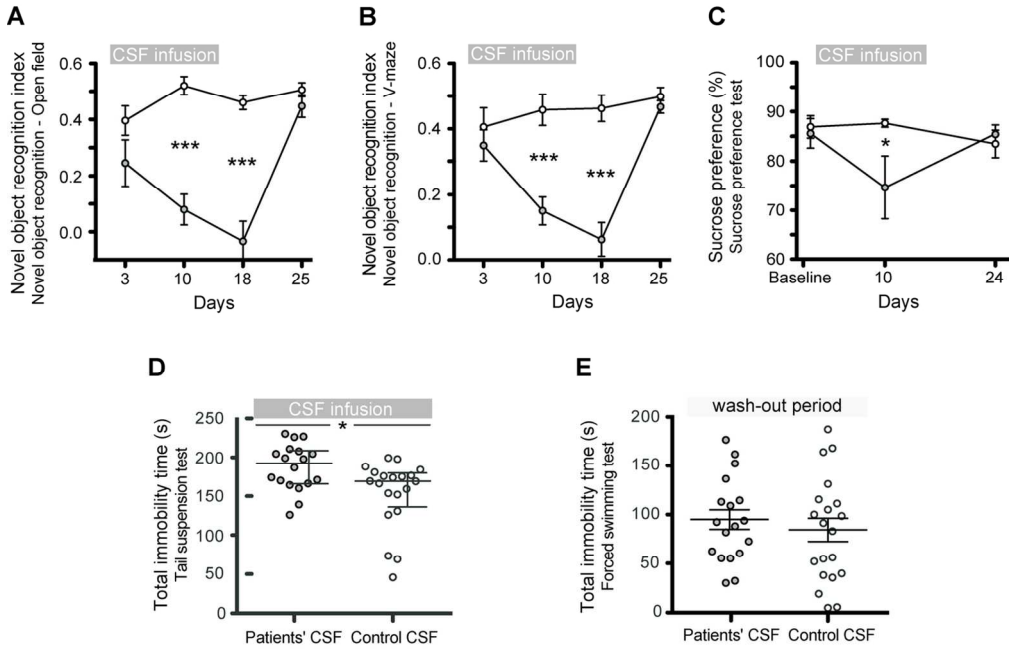

Figure 2: Infusion of CSF from patients with NMDAR antibodies causes deficits in memory, anhedonia, and depressive-like behavior

(A,B) Novel object recognition (NOR) index in open field (A) or V-maze paradigms.

(B) in animals treated with patients' CSF (grey circles) or control CSF (white circles) A high index indicates better object recognition memory.

(C) Preference for sucrose-containing water in animals infused with patients CSF (grey) or control CSF (white). Lower percentages indicate anhedonia.

(D,E) Total time of immobility in tail-suspension test during the infusion period (D, day 12) and in forced swimming test after the infusion period (E, day 20). Data are presented as mean ± s.e.m (median ± IQR in D).

Number of animals: Patients' CSF n=18 (open field NOR n=8), control CSF n=20 (open field NOR n=10). Significance of treatment effect was assessed by two-way ANOVA (A-C) with an α-error of 0.05 and post-hoc testing with Sidak-Holm adjustment (asterisks), unpaired t-test (E) or Mann-Whitney U test (D). * P<0.05, *** P<0.001. See Supplemental Table 1 for detailed statistics.

125x80mm (300 x 300 DPI)

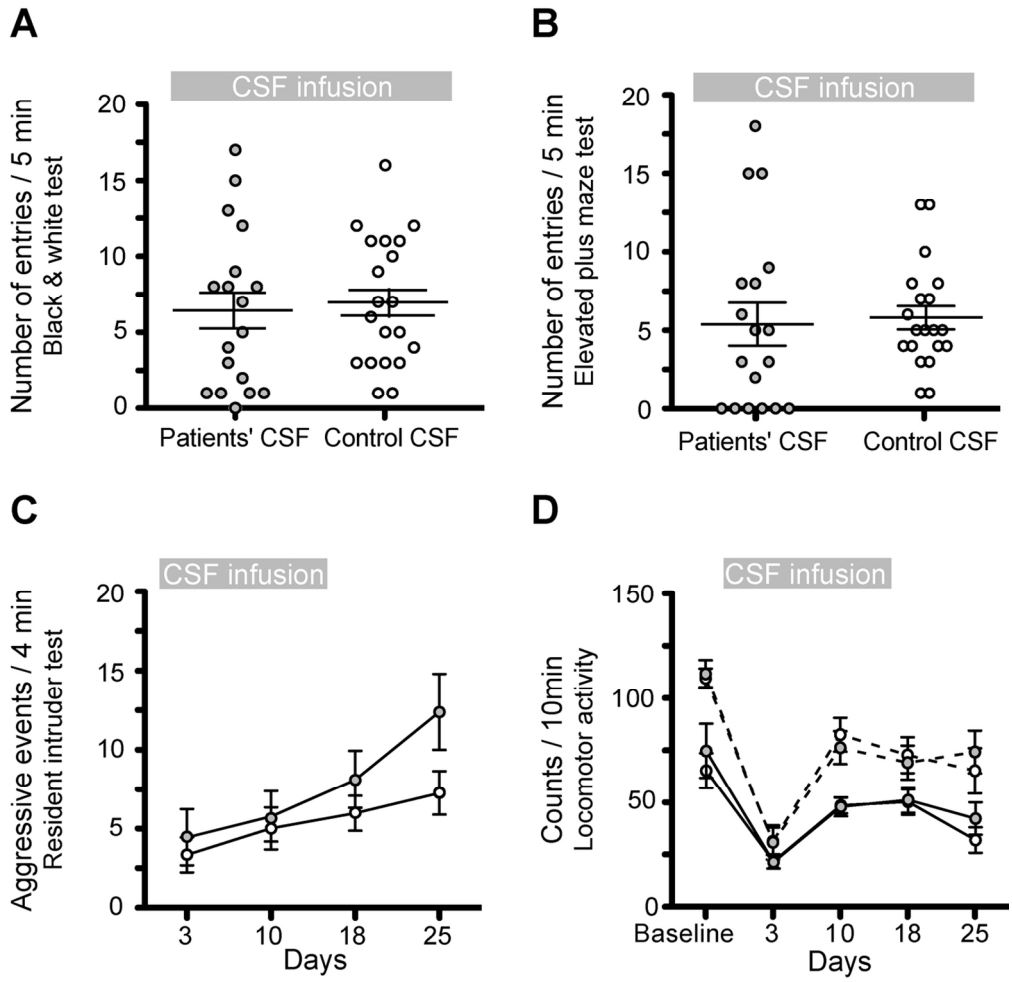

Figure 3: Infusion of CSF from patients with NMDAR antibodies does not alter the tests of anxiety, aggression, and locomotor activity

(A, B) Number of entries into bright/open compartments during a five minute period in a standard black & white (A, day 6) or elevated plus maze test (B, day 14) in animals treated with patients' CSF (grey circles) or control CSF (white circles).

(C) Number of aggressive events over a four-minute period in a resident intruder paradigm in both treatment groups.

(D) Horizontal (solid lines) and vertical (dashed lines) movement count over a ten minute period in both treatment groups.

Data are presented as mean ± s.e.m. Number of animals: Patients' CSF n=18, control CSF n=20. Statistical assessment as indicated in Figure 2, and Supplemental Table 1.

122x119mm (300 x 300 DPI)

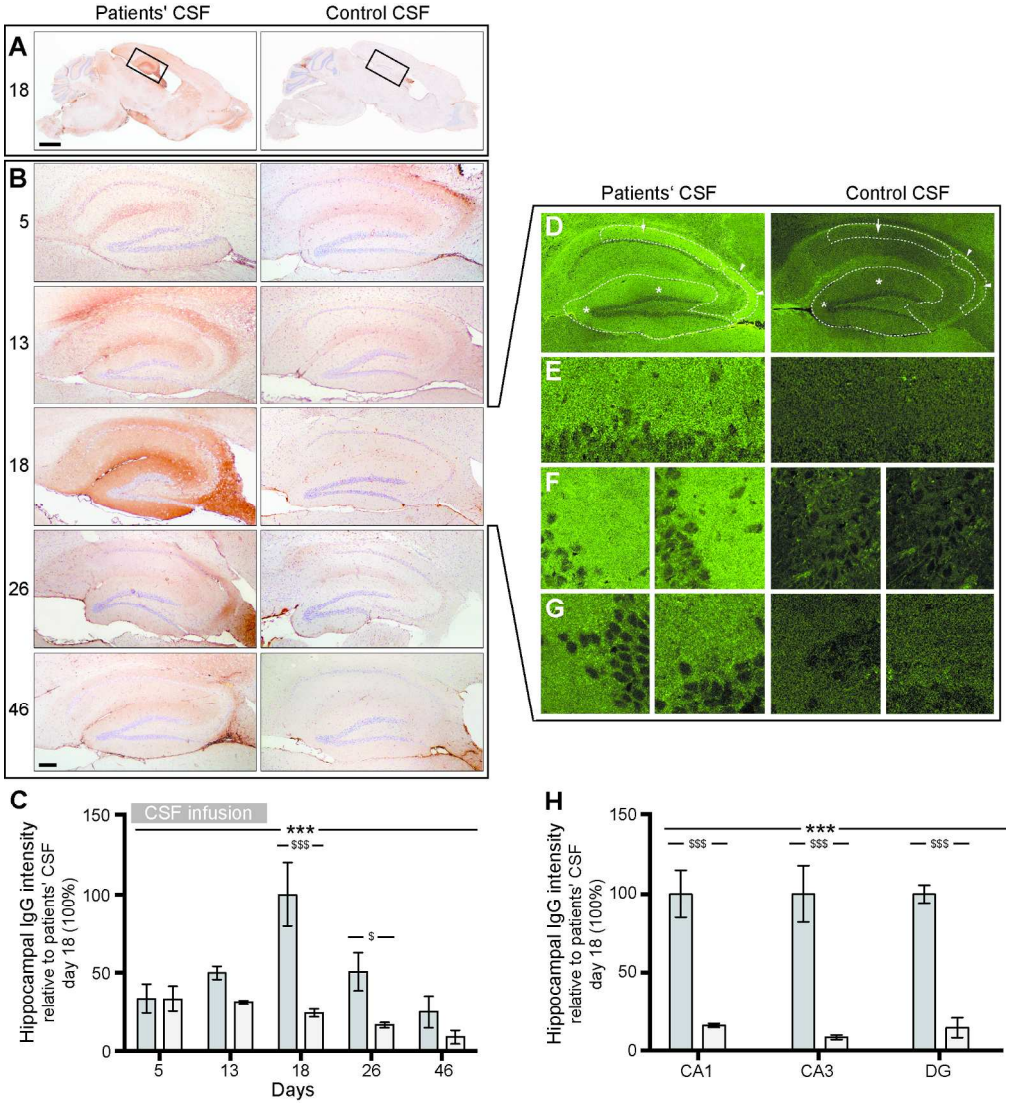

Figure 4: Animals infused with patient's CSF have a progressive increase of human IgG bound to hippocampus

(A, B) Immunostaining of human IgG in sagittal brain sections (A) and hippocampus (B) of representative animals infused with patients' CSF (left panels) and control CSF (right panels), sacrificed at the indicated experimental days. In animals infused with patients' CSF there is a gradual increase of IgG immunostaining until day 18, followed by decrease of immunostaining. Scale bar in A=2 mm; scale bar in B=200 µm.

(C) Quantification of intensity of human IgG immunolabeling in hippocampus of mice infused with patients' CSF (grey columns) and control CSF (white columns) sacrificed at the indicated time points.

(D-H) Confocal microscopy analysis of IgG bound to the hippocampus on day 18. (D) Sagittal section of the hippocampus with areas examined at higher magnification in E (arrow in CA1), F (arrow heads in CA3) and G (asterisks in dentage gyrus [DG]). Note the fine punctate IgG immunolabeling surrounding neuronal bodies in mice infused with patients CSF; this immunolabeling is similar to that reported in brain sections directly incubated with patients' antibodies, as in (Dalmau et al. 2008). Scale bar in D=200 µm; scale bars in E-G=10 µm.

(H) Quantification of the intensity of human IgG immunofluorescence in the indicated areas in animals infused with patients' CSF (grey columns) or control CSF (white columns).

For all quantifications, mean intensity of IgG immunostaining in the group with the highest value (animals

treated with patients' CSF and sacrificed at day 18) was defined as 100%. All data are presented as mean ± s.e.m. For each time point 5 animals infused with patients' CSF and 5 with control CSF were examined. Significance of treatment effect was assessed by two-way ANOVA with an α-error of 0.05 (*) and post-hoc testing with Sidak-Holm adjustment ($). ***, $$$ P<0.001; $, P<0.05. See Supplemental Table 2 for detailed statistics.
186x204mm (300 x 300 DPI)

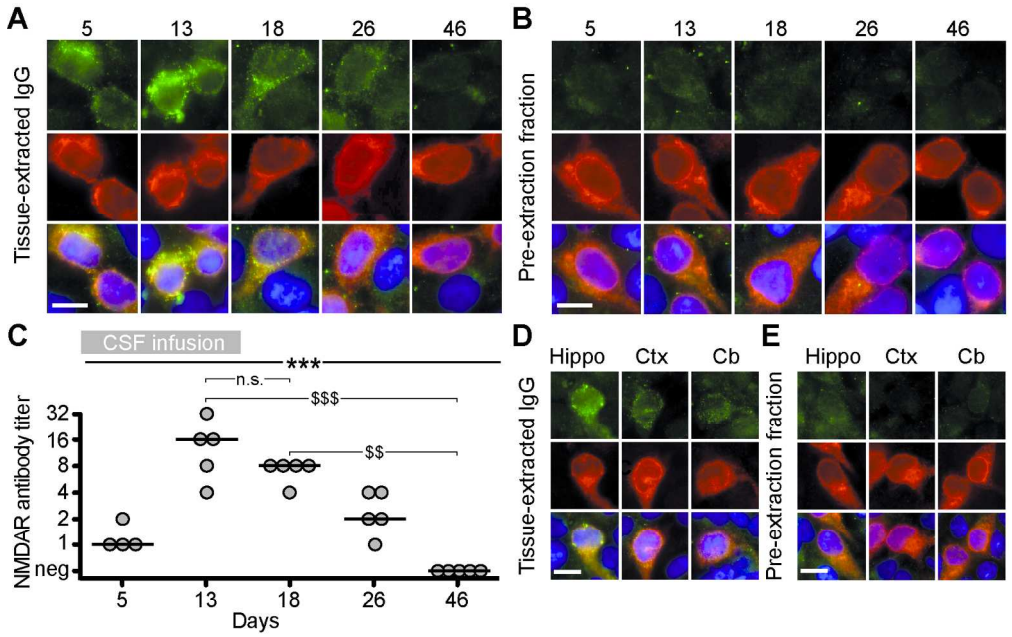

Figure 5: The human IgG extracted from brain of mice infused with patients' CSF is specific for NMDARs (A,B) HEK293 cells expressing the GluN1 subunit of the NMDAR immunolabeled with acid-extracted IgG fractions (top row in A) or pre-extraction fractions (top row in B) from hippocampus of mice infused with patients' CSF and sacrificed on the indicated days. The maximal reactivity with GluN1-expressing cells was noted in acid-extracted IgG fractions from days 13 and 18 (A); none of the pre-extraction fractions showed GluN1 reactivity (B) indicating that the reactivity of acid-extracted fractions corresponds to IgG antibodies that were bound to brain NMDAR receptors. The second row in A and B shows the reactivity with a monoclonal GluN1 antibody, and the third row the co-localization of immunolabeling. Scale bars=10μm. (C) Quantification of NMDAR antibody titer in IgG-extracted fractions from hippocampus of animals treated with patients' CSF (n= 5 mice per each time point, except 4 mice for day 5). Solid line = median. Significance was tested by Kruskal-Wallis with an α-error of 0.05 (asterisks) and post-hoc testing with Dunn's test ($). **,$$ P<0.01, ***,$$$ P<0.001. See Supplemental Table 2 for detailed statistics. (D, E) HEK293 cells expressing the GluN1 subunit of the NMDAR immunolabeled with acid-extracted IgG fractions (D) and pre-extraction fractions (E) from hippocampus, cerebral cortex (Ctx) and cerebellum (Cb) of mice infused with patients' CSF (day 18). The acid-extracted IgG fraction from hippocampus showed higher level of NMDAR antibodies than those extracted from cerebral cortex (ctx) and cerebellum (Cb). Scale bars=10μm.
164x103mm (300 x 300 DPI)

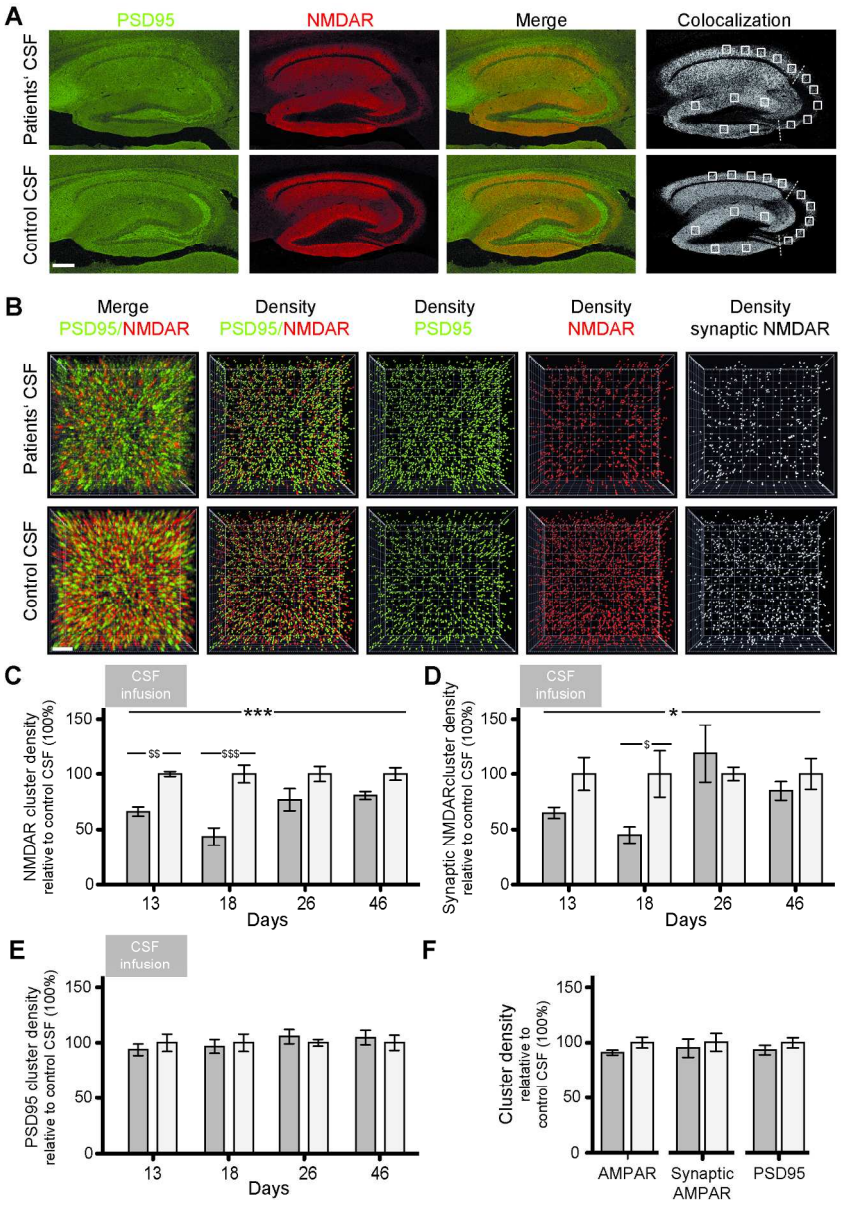

Figure 6: Patients' NMDAR antibodies selectively reduce the density of total and synaptic NMDAR clusters in hippocampus of mice

(A) Hippocampus of mice infused for 14 days (day 18) with patients' CSF (upper row) or control CSF (lower row) immunolabeled for PSD95 and NMDAR. Images were merged (merge) and post-processed to demonstrate co-localizing clusters (colocalization). Squares in "colocalization" indicate the analyzed areas in CA1, CA3 and DG. Scale bar=200 µm.

(B) 3D projection and analysis of the density of total clusters of PSD95 and NMDAR, and synaptic clusters of NMDAR (defined as NMDAR clusters colocalizing with PSD95) in a representative CA3 region (square in A "colocalization"). Merged images (merge, PSD95 green, NMDAR red) were post-processed and used to calculate the density of clusters (density=spots/µm3). Scale bar=2 µm.

(C-F) Quantification of the density of total (C) and synaptic (D) NMDAR clusters, PSD95 clusters (E), and total/synaptic AMPAR clusters (day 18 only, F) in a pooled analysis of hippocampal subregions (CA1, CA3, DG) in animals treated with patients' CSF (grey) or control CSF (white) on the indicated days. Mean density

of clusters in control CSF treated animals was defined as 100%. Data are presented as mean ± s.e.m. For each time point 5 animals infused with patients' CSF and 5 with control CSF were examined. Significance of treatment effect was assessed by two-way ANOVA with an α-error of 0.05 (asterisks) and post-hoc testing with Sidak-Holm adjustment ($) (C,D,E) or unpaired t-test (F). *,$ P< 0.05; **,$$ P< 0.01; ***,$$$ P<0.001. See Supplemental Table 2 for detailed statistics.
161x231mm (300 x 300 DPI)

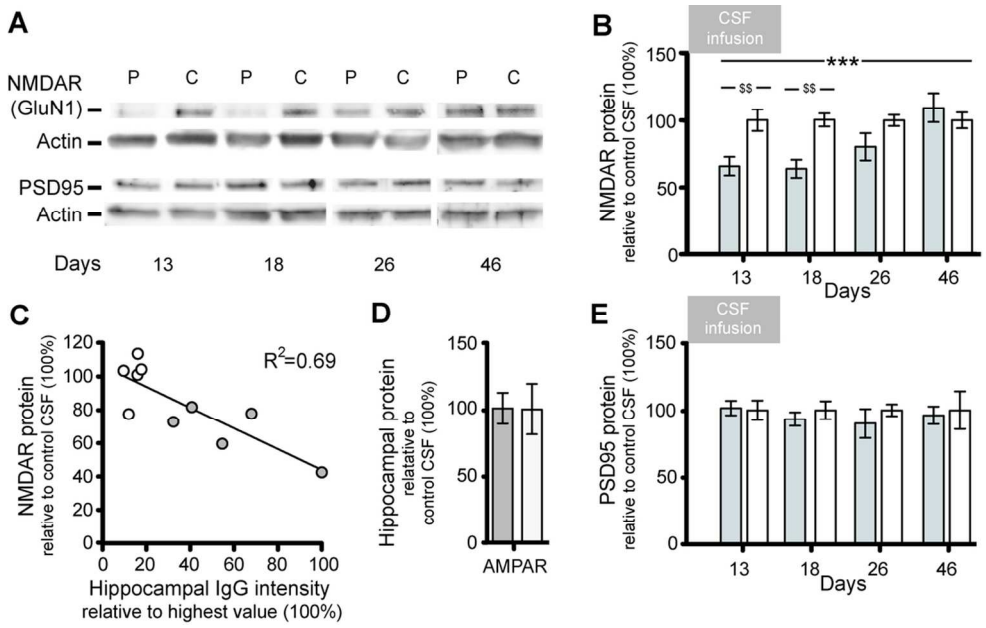

Figure 7: Patients' NMDAR antibodies selectively reduce the protein concentration of NMDAR in hippocampus of mice

A) Representative immunoblots of proteins extracted from hippocampus of animals infused with patients' CSF (P) or control CSF (C) sacrificed at the indicated time points and probed for expression of GluN1 (NMDAR), PSD95 and β-Actin (loading control). Note that there is less visible GluN1 expression on days 13 and 18.

(B, D, E) Quantification of total NMDAR (B), PSD95 (D) or AMPAR (E) protein in animals treated with patients' CSF (grey columns) or control CSF (white columns) sacrificed at the indicated time points (AMPAR day 18 only, E). Results were normalized to β-Actin (loading control). Mean band density of animals treated with control CSF was defined as 100%. Data are presented as mean ± s.e.m. For each time point 6 animals infused with patients' CSF and 6 with control CSF were examined (for days 26 and 46, only 5 animals treated with patient's CSF were available). Significance of treatment effect was assessed by two-way ANOVA with an α-error of 0.05 (asterisks) and post-hoc testing with Sidak-Holm adjustment ($). $$ P< 0.01; *** P< 0.001. See Supplemental Table 2 for detailed statistics

(C) Correlation between concentration of human IgG bound to hippocampus (x-axis, highest hippocampal IgG intensity was defined as 100%) and hippocampal NMDAR protein concentration in mice sacrificed on day 18 (R2=0.69, p=0.003). Grey circles: mice infused with patients' CSF (n=5), white circles: mice infused with control CSF (n=5).

105x65mm (300 x 300 DPI)

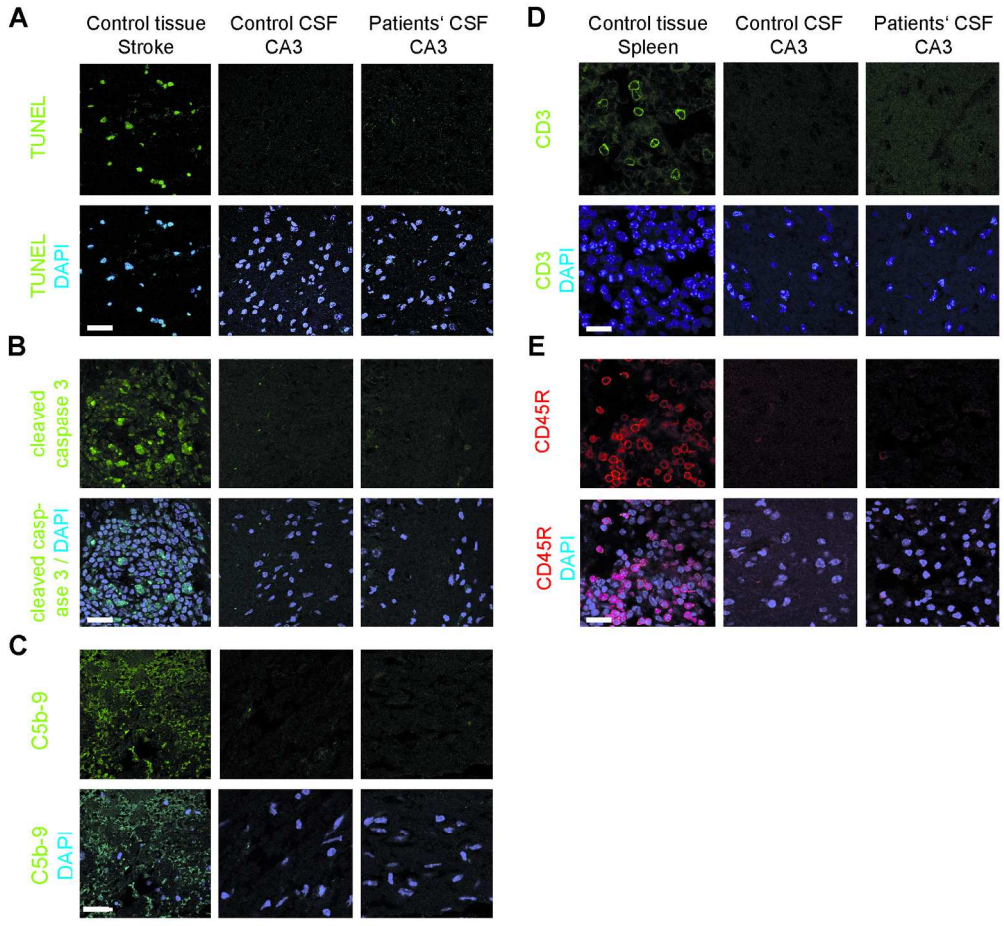

Figure 8: Absence of neuronal apoptosis, deposits of complement, and lymphocytic infiltrates in the hippocampus of mice infused with patients' CSF

(A,B) TUNEL and cleaved caspase 3 immunolabeling of a representative area of CA3 (area with maximal IgG binding and lower NMDAR concentration) of an animal infused with patients CSF, showing lack of apoptotic cells. A section of the same region in an animal with transient middle cerebral artery occlusion (stroke model) shows apoptotic cells in the penumbra (panel on the left).

(C) Same CA3 region as in (A) immunostained for C5b-9 showing lack of deposit of complement. A section of the same region in the indicated stroke model shows presence of complement in the penumbra (panel on the left).

(D,E) Same CA3 region as in (A) immunostained for T (CD3) and B (CD45R) lymphocytes showing absence of inflammatory infiltrates. A section of spleen was used as control tissue showing the presence of CD3 (green) and CD45R (red) cells. Scale bar=10 µm. Total number of animals examined: patients' CSF n=5; control CSF n=5. Scale bars=20µm.

180x168mm (300 x 300 DPI)

Supplemental material

Behavioral animal tests and references

Supplemental Tables 1 and 2

Supplemental Figures 1 and 2

Behavioral animal tests

Novel object recognition (NOR) test: This test was performed in two paradigms, open field (45x45x40 cm, Panlab, Spain) and in V-maze (40 cm per side, Panlab, Spain) using two different groups of animals, as reported by us and others [Bura *et al.* 2007;Taglialatela *et al.* 2009;Puighermanal *et al.* 2009]. On day 1 (same day of osmotic pump implantation, before surgery) mice were habituated for 30 minutes in the open field arena, or 9 minutes in the V-maze. On days 3, 10, 18 and 25, mice were put back into the open field arena or into the V-maze for 9 minutes; two identical objects were presented, and the time the mice spent exploring each object was recorded. After a retention phase of 3 hours, the mice were placed for another 9 minutes into the open field arena or into the V-maze; in each paradigm one of the familiar objects was replaced with a novel object and the total time spent exploring each object (novel and familiar) was registered. During the test phase of the open field paradigm, the objects were positioned in the opposite corners of those used in the training phase and the novel object was presented in 50% of trials on the right and in 50% of trials on the left side. Object exploration was defined as the orientation of the nose to the object at a distance of less than 2 cm. A discrimination index was calculated as the difference of the time spent exploring the novel and the time spent exploring the familiar object divided by the total time exploring both objects. A

higher discrimination index is considered to reflect greater memory retention for the familiar object [Puighermanal, Marsicano, Busquets-Garcia, Lutz, Maldonado, and Ozaita2009;Ennaceur 2010].

Sucrose preference test: This test was performed on days 10 and 24 after surgery, as previously reported [Bura *et al.* 2013;Strekalova *et al.* 2006]. During the 4 days preceding surgery, two bottles of water, one with 2% sucrose and the other without, were placed in the cage. Every day the position of the bottles was exchanged, and the consumption from each bottle measured. On the day of the test, the two bottles were placed again in the cage and the consumption from each recorded after a 24h interval. The preference for sucrose was calculated as the relative amount of water with sucrose versus total liquid (water with and without sucrose) consumed by the mice.

Tail suspension test (TST): This test was performed on day 12 after surgery, as previously reported [Steru *et al.* 1985;Aso *et al.* 2008]. Mice were suspended 50 cm above a solid surface by the use of adhesive tape applied to the tail (3/4 of the distance from the base of mouse tail). During a six minutes interval, the total time of immobility was recorded. Long periods of immobility are characteristic of a depressive-like state; an alternative test is the forced swimming test, which was also applied at a different time point (see below).

Forced swimming test (FST): This test was performed on day 20 after surgery, as previously reported [Filliol *et al.* 2000;Porsolt *et al.* 1977]. The mouse was placed in a plastic cylinder containing warm water (27-28 °C), deep enough to prevent touching the bottom of the cylinder and forcing the mouse to swim. The trial lasted 6 minutes and the total time of immobility after

minute 2:00 was recorded. Time of immobility was defined as the time that the animal stopped swimming and only used minimal movements to keep the head above the water.

Black and white test: This test was performed on day 6 after surgery, as reported [Bura *et al.* 2010;Crawley and Goodwin 1980]. It measures the conflict between the natural tendency of rodents to explore new environments and the tendency to avoid brightly illuminated areas. The box consisted of two compartments (20 cm wide × 20 cm long × 30 cm high) connected by a 6 cm wide by 6 cm high tunnel. One compartment was painted black and maintained at 10 lux, while the other compartment was painted white, brightly illuminated (500 lux), and subdivided into three sections (distal, medial and proximal), based on the distance from the tunnel. The floor of both compartments was subdivided into squares (5x5 cm) to measure the locomotor activity. At the start of the session, mice were placed in the black compartment, head facing a corner. The latency of first entry into the white compartment and section reached in each entry, together with time spent, squares crossed, and number of entries into both compartments were recorded and used to evaluate anxiety.

Elevated plus maze test: This test was performed on day 14 after surgery, as reported [Handley and Mithani 1984;Llorente-Berzal *et al.* 2013]. The test is based on the same principle as the black and white test, and measures the conflict between the natural tendency of mice to avoid an illuminated and elevated surface, and the natural tendency to explore new environments. It consisted of a plastic black cross with arms 40 cm long and 6 cm wide placed 50 cm above the floor. Two opposite arms were surrounded by walls (15 cm high, closed arms, 10 lux), while the two other arms were devoid of such walls (open arms, 200 lux). The four arms were connected

by a central platform. At the start of the session, the mouse was placed at the end of a closed arm facing the wall. During the 5-minute trial, the number of entries and the time spent in each arm were recorded. Anxiety was assessed as both the time spent avoiding the open arms and the number of entries into them.

Resident-intruder test: This test, performed on days 3, 10, 18 and 25 after surgery, evaluates aggressive behavior in rodents, as reported [Konig *et al.* 1996;Burokas *et al.* 2012]. Resident mice were housed individually for at least 10 days before the test. Intruder animals of similar age and weight were housed five per cage. Each session consisted of putting together resident and intruder mice for a period of 4 minutes, measuring the latency of the first aggressive event and frequency of events.

Locomotor activity: This test was performed on days 3, 10, 18 and 25 after surgery. Animals were assessed in locomotor activity boxes (9×20×11 cm; Imetronic, Passac, France), equipped with 2 rows of photocell detectors, and placed in a low-luminosity environment (20–25 lux), as previously described [Caille *et al.* 1999;Berrendero *et al.* 2005]. The mouse locomotor activity was recorded for 10 minutes as horizontal activity and vertical activity.

Legends to supplemental figures

Supplemental Figure 1: Quantification of human IgG present in mice cerebral cortex

Quantification of the intensity of immunolabeling of human IgG present in frontal cortex of mice infused with patients' CSF (grey columns) or control CSF (white columns) sacrificed at the indicated time points. The change over time of the amount of patients' IgG detected in frontal cortex is similar to that demonstrated in hippocampus (see Figure 4 C: progressive increase until day 18 followed by a wash out period). Note that despite the similarity in the dynamics of patient's IgG detection, in all time points the amount of patients' IgG in frontal cortex was substantially less than that found in hippocampus (5% versus 100%)

Mean intensity of immunostaining of patients' IgG detected in hippocampus in the group with the highest value (animals infused with patients' CSF examined at day 18) was defined as 100%. All data are presented as mean ± s.e.m. For each time point 5 animals infused with patients' CSF and 5 with control CSF were examined. Significance of treatment effect was assessed by two-way ANOVA with an α-error of 0.05 (*) and post-hoc testing with Sidak-Holm adjustment ($). ***, $$$ $P<0.001$; $, $P<0.05$.

Supplemental Figure 2: Abscence of brain-bound NMDAR-specific IgG in mice infused with CSF from NMDAR antibody negative patients (control)

HEK293 cells expressing the GluN1 subunit of the NMDAR immunolabeled with acid-extracted IgG fractions (top row) from hippocampus of mice infused with control CSF and sacrificed on the indicated days. No reactivity is observed. The second row shows the reactivity with a monoclonal GluN1 antibody, and the third row the co-localization of immunolabeling. Scale bars=10µm.

References

Aso E, Ozaita A, Valdizan EM *et al*. BDNF impairment in the hippocampus is related to enhanced despair behavior in CB1 knockout mice. J Neurochem 2008; 105: 565-572.

Berrendero F, Mendizabal V, Robledo P *et al*. Nicotine-induced antinociception, rewarding effects, and physical dependence are decreased in mice lacking the preproenkephalin gene. J Neurosci 2005; 25: 1103-1112.

Bura AS, Guegan T, Zamanillo D, Vela JM, Maldonado R. Operant self-administration of a sigma ligand improves nociceptive and emotional manifestations of neuropathic pain. Eur J Pain 2013; 17: 832-843.

Bura SA, Burokas A, Martin-Garcia E, Maldonado R. Effects of chronic nicotine on food intake and anxiety-like behaviour in CB(1) knockout mice. Eur Neuropsychopharmacol 2010; 20: 369-378.

Bura SA, Castane A, Ledent C, Valverde O, Maldonado R. Genetic and pharmacological approaches to evaluate the interaction between the cannabinoid and cholinergic systems in cognitive processes. Br J Pharmacol 2007; 150: 758-765.

Burokas A, Gutierrez-Cuesta J, Martin-Garcia E, Maldonado R. Operant model of frustrated expected reward in mice. Addict Biol 2012; 17: 770-782.

Caille S, Espejo EF, Reneric JP, Cador M, Koob GF, Stinus L. Total neurochemical lesion of noradrenergic neurons of the locus ceruleus does not alter either naloxone-precipitated or spontaneous opiate withdrawal nor does it influence ability of clonidine to reverse opiate withdrawal. J Pharmacol Exp Ther 1999; 290: 881-892.

Crawley J, Goodwin FK. Preliminary report of a simple animal behavior model for the anxiolytic effects of benzodiazepines. Pharmacol Biochem Behav 1980; 13: 167-170.

Ennaceur A. One-trial object recognition in rats and mice: methodological and theoretical issues. Behav Brain Res 2010; 215: 244-254.

Filliol D, Ghozland S, Chluba J *et al*. Mice deficient for delta- and mu-opioid receptors exhibit opposing alterations of emotional responses. Nat Genet 2000; 25: 195-200.

Handley SL, Mithani S. Effects of alpha-adrenoceptor agonists and antagonists in a maze-exploration model of 'fear'-motivated behaviour. Naunyn Schmiedebergs Arch Pharmacol 1984; 327: 1-5.

Konig M, Zimmer AM, Steiner H *et al*. Pain responses, anxiety and aggression in mice deficient in pre-proenkephalin. Nature 1996; 383: 535-538.

Llorente-Berzal A, Puighermanal E, Burokas A *et al*. Sex-dependent psychoneuroendocrine effects of THC and MDMA in an animal model of adolescent drug consumption. PLoS ONE 2013; 8: e78386.

Porsolt RD, Bertin A, Jalfre M. Behavioral despair in mice: a primary screening test for antidepressants. Arch Int Pharmacodyn Ther 1977; 229: 327-336.

Puighermanal E, Marsicano G, Busquets-Garcia A, Lutz B, Maldonado R, Ozaita A. Cannabinoid modulation of hippocampal long-term memory is mediated by mTOR signaling. Nat Neurosci 2009; 12: 1152-1158.

Steru L, Chermat R, Thierry B, Simon P. The tail suspension test: a new method for screening antidepressants in mice. Psychopharmacology (Berl) 1985; 85: 367-370.

Strekalova T, Gorenkova N, Schunk E, Dolgov O, Bartsch D. Selective effects of citalopram in a mouse model of stress-induced anhedonia with a control for chronic stress. Behav Pharmacol 2006; 17: 271-287.

Taglialatela G, Hogan D, Zhang WR, Dineley KT. Intermediate- and long-term recognition memory deficits in Tg2576 mice are reversed with acute calcineurin inhibition. Behav Brain Res 2009; 200: 95-99.

Supplemental Table 1: Statistical analysis of cognitive and memory tests

		2way ANOVA analysis				Post-hoc analysis				
	Test	Variable	Source of variation	Uncorrected P-value	F-value	Day	Mean patients' CSF	Mean control CSF	Difference	Multiplicity-adjusted P-value[&]
Memory	Novel object recognition - open field	Novel object recognition index	Time	<0.001	9.96	3	0.25	0.40	-0.15	0.066
			Treatment	**<0.001**	67.5	10	0.08	0.52	-0.44	**<0.001**
			Interaction	**<0.001**	9.45	18	-0.03	0.46	-0.49	**<0.001**
						25	0.45	0.51	-0.06	0.40
		Total time of exploration (Internal control)	Time	0.003	5.48					
			Treatment	0.37	0.86					
			Interaction	0.18	1.76					
	Novel object recognition - V-maze	Novel object recognition index	Time	<0.001	12.6	3	0.35	0.41	-0.056	0.066
			Treatment	**<0.001**	24.2	10	0.15	0.46	**-0.31**	**<0.001**
			Interaction	**<0.001**	11.3	18	0.06	0.26	**-0.40**	**<0.001**
						25	0.47	0.50	-0.031	0.40
		Total time of exploration (Internal control)	Time	<0.001	14.8					
			Treatment	0.39	0.76					
			Interaction	0.37	1.07					
Anhedonia	Sucrose preference test	Percentage of sucrose preference	Time	0.30	1.22	-4 to 0	85.60	86.92	-1.33	0.89
			Treatment	0.10	2.87	10	74.64	87.66	-13.02	**0.016**
			Interaction	**0.068**	2.82	24	85.40	83.47	1.93	0.89
		Total fluid consumption (Internal control)	Time	<0.001	10.1					
			Treatment	0.50	0.46					
			Interaction	0.87	0.14					
Locomotion	Locomotor activity test	Horizontal Activity	Time	<0.001	14.6					
			Treatment	0.40	0.73					
			Interaction	0.85	0.34					
		Vertical Activity	Time	<0.001	39.0					
			Treatment	0.98	0.001					
			Interaction	0.80	0.41					
Aggressiveness	Resident-instruder test	Frequency	Time	<0.001	7.08					
			Treatment	0.16	2.04					
			Interaction	0.36	1.07					
		Latency of aggressive events	Time	0.46	0.85					
			Treatment	0.29	1.14					
			Interaction	0.98	0.068					

	Unpaired t-test / Mann Whitney-U test				
	Test, Day	Variable	mean patients' CSF (95% CI)	mean control CSF (95% CI)	Uncorrected P-value
Depression	Tail suspension test day 12	Time of immobility	169.2 (136.2-179.8)*	192.4 (165.8-208.7)*	**0,017***
	Forced swimming test day 20	Time of immobility	93.8 (72.5-115)	83.1 (58.0-108)	0.50
Anxiety	Black and white test day 6	Latency	67.8 (21.1-114)	29.2 (8.41-50.1)	0.25
		% Time in white box	12.4 (6.58-18.3)	14.9 (9.99-19.7)	0.19
		Entries in white box	6.39 (3.77-9.01)	7.00 (5.00-9.00)	0.70
		Entries in distal section	2.94 (1.46-4.43)	3.35 (2.20-4.50)	0.46
	Elevated plus maze test day 14	% Time in open arms	6.27 (2.18-10.4)	6.75 (4.12-9.38)	0.15
		Entries in open arms	5.39 (2.51-8.26)	5.80 (4.24-7.36)	0.79

In the 2-way ANOVA analysis a p-value of 0.05 is considered significant for the treatment effect. An interaction p-value < 0.10 is considered a sign of different treatment effects at different time points, warranting post-hoc analysis. Significant results for treatment effect or interaction of treatment and time are shown in bold. * Median, IQR and result of significance testing using Mann Whitney-U test indicated because of non-normality. [&] Multiplicity-adjusted P-value using Sidak-Holm post-hoc procedure.

Supplemental Table 2: Statistical analysis of human IgG and receptor studies

	2way ANOVA analysis				Post-hoc analysis				
Test	*Variable*	*Source of variation*	*P-value*	*F-value*	*Day*	*Mean patients' CSF*	*Mean control CSF*	*Difference*	*Multiplicity-adjusted P-value* [&]
Immuno-histo-chemistry (Figure 4)	Human IgG intensity in hippocampus – Percent of patients' CSF treated animals (100%)	Time	**0.0005**	6.23	3	33.6	33.3	0.28	0.98
		Treatment	**<0.0001**	24.7	10	49.9	31.4	18.5	0.42
					18	100.0	24.0	76.0	**<0.0001**
		Interaction	**0.003**	4.89	25	50.7	16.4	34.4	**0.048**
					46	25.0	8.84	16.1	0.42
Immuno-fluores-cence (Figure 4)	Human IgG intensity in hippocampus - Percent of patients' CSF treated animals (100%)	Region	0.93	0.077	CA1	100.0	16.0	84.1	**<0.0001**
		Treatment	**<0.0001**	109.2	CA3	100.0	8.38	91.6	**<0.0001**
		Interaction	0.93	0.077	DG	100.0	14.4	85.6	**<0.0001**
Confocal cluster density (Figure 6)	NMDAR - Percent of control CSF treated animals (100%)	Time	**0.032**	3.30	13	66.2	100.0	33.8	**0.004**
		Treatment	**<0.0001**	51.8	18	43.4	100.0	56.6	**<0.0001**
		Interaction	**0.032**	3.30	26	76.8	100.0	23.2	0.054
					46	80.8	100.0	19.2	0.18
	Synaptic NMDAR - Percent of control CSF treated animals (100%)	Time	0.086	2.40	13	65.0	100.0	35.0	0.33
		Treatment	**0.039**	2.40	18	44.9	100.0	55.1	**0.044**
		Interaction	**0.086**	4.60	26	118.5	100.0	-18.5	0.82
					46	84.8	100.0	15.3	0.92
	PSD95 - Percent of control CSF treated animals (100%)	Time	0.73	1.13					
		Treatment	0.97	0.028					
		Interaction	0.73	1.13					
Total protein - Immuno-blot (Figure 7)	NMDAR GluN1 - Percent of control CSF treated animals (100%)	Time	0.022	3.63	13	65.6	100.0	34.4	**0.0082**
		Treatment	**0.0008**	13.2	18	63.7	100.0	36.3	**0.0067**
		Interaction	**0.022**	3.63	26	80.3	100.0	19.7	0.19
					46	110.0	100.0	-9.54	0.40
	PSD95 - Percent of control CSF treated animals (100%)	Time	0.91	0.18					
		Treatment	0.43	0.64					
		Interaction	0.91	0.18					

Kruskal-Wallis analysis				Post-hoc analysis				
Test	Variable	P-value	Test statistic	Pairwise Day	Mean rank 1	Mean rank 2	Difference	P[@]
IgG extraction hippo-campus (Figure 5)	NMDAR antibody titer	**0.0004**	20.6	46 vs. 5	3	8.38	-5.38	1.0
				46 vs. 13	3	20.5	-17.5	**0.0004**
				46 vs. 18	3	18.1	-15.1	**0.0031**
				46 vs. 26	3	11.7	-8.7	0.24
				13 vs. 18	18.1	20.5	-2.4	1.0

Unpaired t-test				
Test	*Variable*	*mean patients' CSF (95% CI)*	*mean control CSF (95% CI)*	*Uncorrected P-value*
Confocal cluster density (Figure 6)	AMPAR - Percent of control CSF treated animals (100%)	90.9 (84.6-97.2)	100.0 (86.6-113.5)	0.14
	Synaptic AMPAR - Percent of control CSF treated animals (100%)	94.8 (71.6-118.0)	100.0 (77.8-122.2)	0.66
	PSD95 - Percent of control CSF treated animals (100%)	93.4 (82.4-104.4)	100.0 (86.9-113.1)	0.33
Immuno-blot (Figure 7)	AMPAR - Percent of control CSF treated animals (100%) - day 18	106.5 (76.4-136.5)	100.0 (58.5-151.5)	0.75

In the 2-way ANOVA analysis a p-value of 0.05 is considered significant for the treatment effect. An interaction p-value < 0.10 is considered a sign of different treatment effects at different time points, warranting post-hoc analysis. Significant results for treatment effect or interaction of treatment and time are shown in bold. [&]Multiplicity-adjusted P-value using Sidak-Holm post-hoc procedure. [@]Multiplicity-adjusted P-value by Dunn's post-hoc procedure.

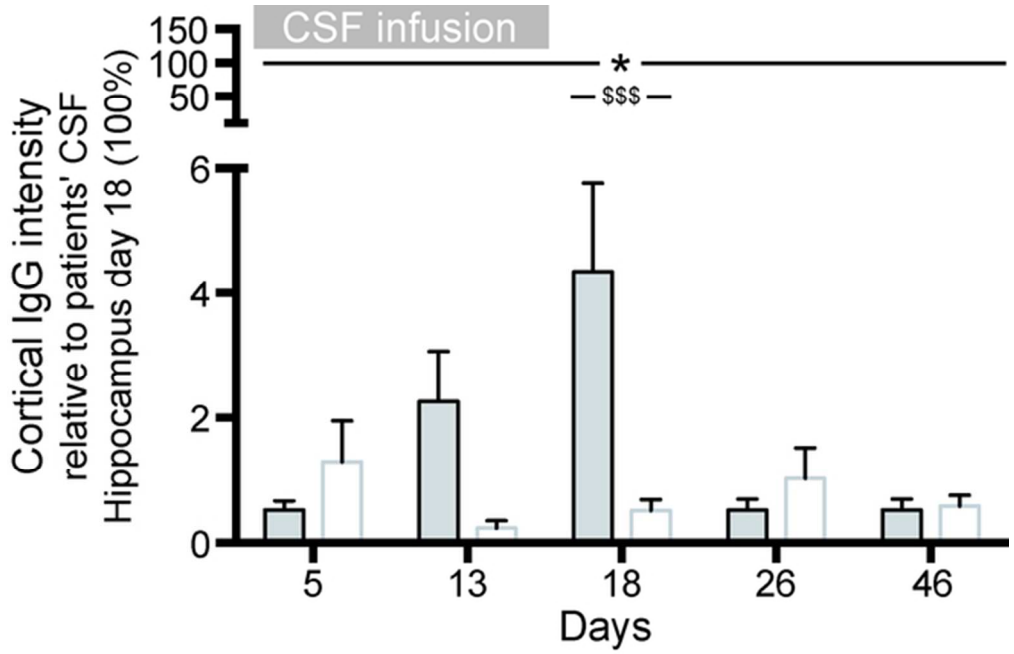

Supplemental Figure 1: Quantification of human IgG present in mice cerebral cortex
Quantification of the intensity of immunolabeling of human IgG present in frontal cortex of mice infused with patients' CSF (grey columns) or control CSF (white columns) sacrificed at the indicated time points. The change over time of the amount of patients' IgG detected in frontal cortex is similar to that demonstrated in hippocampus (see Figure 4 C: progressive increase until day 18 followed by a wash out period). Note that despite the similarity in the dynamics of patient's IgG detection, in all time points the amount of patients' IgG in frontal cortex was substantially less than that found in hippocampus (5% versus 100%)
Mean intensity of immunostaining of patients' IgG detected in hippocampus in the group with the highest value (animals infused with patients' CSF examined at day 18) was defined as 100%. All data are presented as mean ± s.e.m. For each time point 5 animals infused with patients' CSF and 5 with control CSF were examined. Significance of treatment effect was assessed by two-way ANOVA with an α-error of 0.05 (*) and post-hoc testing with Sidak-Holm adjustment ($). $$$ P<0.001; $ P<0.05.

55x36mm (300 x 300 DPI)

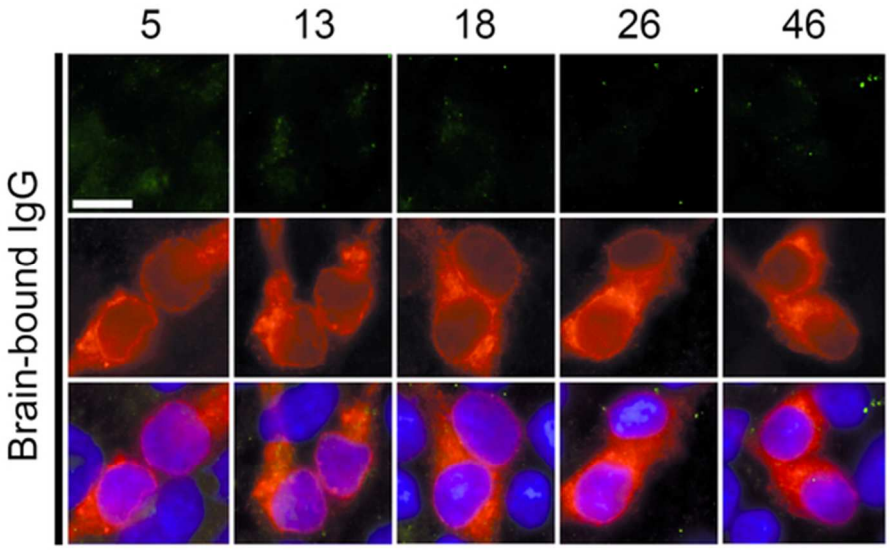

Supplemental Figure 2: Abscence of brain-bound NMDAR-specific IgG in mice infused with CSF from NMDAR antibody negative patients (control)
HEK293 cells expressing the GluN1 subunit of the NMDAR immunolabeled with acid-extracted IgG fractions (top row) from hippocampus of mice infused with control CSF and sacrificed on the indicated days. No reactivity is observed. The second row shows the reactivity with a monoclonal GluN1 antibody, and the third row the co-localization of immunolabeling. Scale bars=10μm.
54x32mm (300 x 300 DPI)